10721
NACA TN 4377

TECH LIBRARY KAFB, NM
0067149

NATIONAL ADVISORY COMMITTEE FOR AERONAUTICS

TECHNICAL NOTE 4377

USE OF THE COANDA EFFECT FOR JET DEFLECTION AND VERTICAL LIFT WITH MULTIPLE-FLAT-PLATE AND CURVED-PLATE DEFLECTION SURFACES

By Uwe H. von Glahn

Lewis Flight Propulsion Laboratory
Cleveland, Ohio

Washington
September 1958

AFMDC
TECHN

TECH LIBRARY KAFB, NM

0067149

NATIONAL ADVISORY COMMITTEE FOR AERONAUTICS

TECHNICAL NOTE 4377

USE OF THE COANDA EFFECT FOR JET DEFLECTION AND VERTICAL LIFT WITH MULTIPLE-FLAT-PLATE AND CURVED-PLATE DEFLECTION SURFACES

By Uwe H. von Glahn

4807

CU-1

SUMMARY

The ratios of lift and axial thrust to undeflected thrust of nozzle-deflection-plate configurations using the Coanda effect for obtaining jet deflection and lift were evaluated from force measurements. Pressure distributions were also obtained over the surfaces of the deflection plates. The convergent nozzles used in the study were of rectangular cross section with exit heights ranging from 0.5 to 2.0 inches. The jet-deflection plates used included configurations made up of two, three, six, and nine flat plates and several curved plates with various radii of curvature, all having side plates equal in height to the nozzle. The nozzles discharged into quiescent air over a range of pressure ratios from 1.5 to 3.0.

In general, the ratio of lift to undeflected thrust of the Coanda nozzles studied was less, depending on the particular configuration, than that theoretically calculated for multiple-flat-plate and curved-plate flaps immersed in an airstream. By use of a configuration made up of nine flat plates and for a 90° angular deflection of the jet stream, a maximum ratio of lift to undeflected thrust near 0.88 was obtained together with zero axial thrust. For a similar jet-deflection angle, the best curved-plate configuration studied achieved a ratio of lift to undeflected thrust of about 0.81. The decrease in the measured ratio of lift to undeflected thrust from that calculated theoretically for a perfect curved plate is attributed to the following factors: (1) pressure and momentum losses in the real jet stream that are not accounted for in theory, (2) the inability of the jet stream to turn the full deflection angle prescribed by the deflection plate, and (3) the fact that optimum designs for the multiple-flat-plate and especially for the curved-plate configurations were not necessarily achieved in the time available for these exploratory studies.

INTRODUCTION

The Coanda effect may be described as the phenomenon by which the proximity of a surface to a jet stream will cause the jet to attach itself to and follow the surface contour (ref. 1). The local pressures on the deflecting surface are less than ambient air pressure; consequently, when the deflecting surface is inclined toward the ground, these negative pressures result in a lift component. A drag component constituting a thrust reduction in the axial-thrust direction is also obtained.

4807

The use of the Coanda effect for obtaining jet-stream deflection and vertical lift from a single-flat-plate deflector is described in reference 2. The data presented in reference 2 show that ratios of lift to undeflected thrust and axial thrust to undeflected thrust comparable to those obtained theoretically with a flat-plate type of mechanical deflector can be achieved. However, the deflection angles for which theoretical values of ratio of lift to undeflected thrust can be obtained with a single-flat-plate deflector are limited by considerations of nozzle height and deflection-plate length.

The negative pressures on a flat plate decrease with progressively increasing distance along the deflection plate; however, with each angle increase of the surface relative to the jet stream, an increase in the negative pressures is again obtained on the deflection surface (ref. 1). Because of this phenomenon, the use of multiple flat plates or a curved surface provides deflection angles and ratios of lift to undeflected thrust much greater than those with single-flat-plate configurations (ref. 3).

The exploratory study reported herein, conducted at the NACA Lewis laboratory, is concerned with the flow and performance characteristics associated with multiple-flat-plate and curved-plate jet-deflecting surfaces. Experimental ratios of lift to undeflected thrust were obtained for configurations yielding jet-stream deflection angles up to about 90° and ratios of axial thrust to undeflected thrust near zero. Data were also obtained on the effect of the relative angle between adjacent flat deflection plates on the ratio of lift to undeflected thrust and local surface pressure distributions over the plates. As in reference 2, rectangular nozzles of simple convergent design rather than conventional circular nozzles were used. The studies were conducted with a small-scale setup (equivalent nozzle-exit diameter less than 2.75 in.) using unheated air and operating at pressure ratios across the nozzle (ratio of absolute jet total pressure to ambient pressure) from 1.5 to 3.0. All data were obtained by discharging the jet into still air at approximately sea-level atmospheric conditions.

The estimated performance of multiple-flat-plate deflectors is discussed in appendix B by Thomas F. Gelder.

4807

CU-1 back

APPARATUS

Test Facility

The test stand used to support the nozzle configurations and to obtain thrust and lift measurements is shown schematically in figure 1. The test stand consisted of a plenum section (inside diam., 3 in.; length, 16.5 in.) mounted horizontally on a link-supported force-measuring system. Unheated air at approximately 50° F was supplied to the plenum by 2.5-inch-inside-diameter twin supply lines (fig. 2). These lines were placed diametrically opposite one another and at right angles to the plenum in order to eliminate possible side and thrust forces caused by the entering air. The lines were also isolated from the force-measuring system by flexible couplings at each end of the supply lines. The nozzles were bolted to a flange at the downstream end of the plenum section. A single total-pressure probe mounted just inside the nozzle-exit plane was used to measure the total pressure of the jet stream.

The net thrust obtained with the nozzle configurations was measured by strain gages mounted near the upstream end of the plenum section (fig. 1). The strain gages on the vertical support link under the nozzle flange were used to measure gross values of vertical or lift forces. The force measurements obtained with these strain gages were recorded on a modified flight recorder.

Coanda Nozzles

A Coanda nozzle consisted of a convergent rectangular nozzle exit, jet-stream deflection plate, and side plates. The nozzles were of a simple convergent design, with no effort being made to achieve an optimum exhaust-nozzle thrust coefficient. The nozzles were formed by flattening progressively a 2.9-inch-diameter tube to a rectangular exit cross section with a desired nozzle height. The exit corners had radii of the order of 0.03 inch. Vertical and horizontal cross sections at the centerline of the nozzles, together with pertinent dimensions, are presented in figure 3.

The jet-stream deflection surfaces consisted of (1) combinations of two, three, six, and nine flat plates, and (2) several curved-plate deflectors.

Multiple-flat-plate deflection surfaces. - For the two- and three-flat-plate configurations, the plates were attached to the nozzle by means of a piano hinge, and each succeeding plate was similarly attached to its adjacent plate (fig. 4). Individual telescoping tubes supported the downstream end of each plate. These supporting tubes were attached to a bracket, which in turn was secured to the nozzle flange. The

deflection angle of each plate was varied independently of the other plates in the configuration. The following schematic sketch shows the general arrangement for the two- and three-flat-plate configurations and identifies the pertinent components:

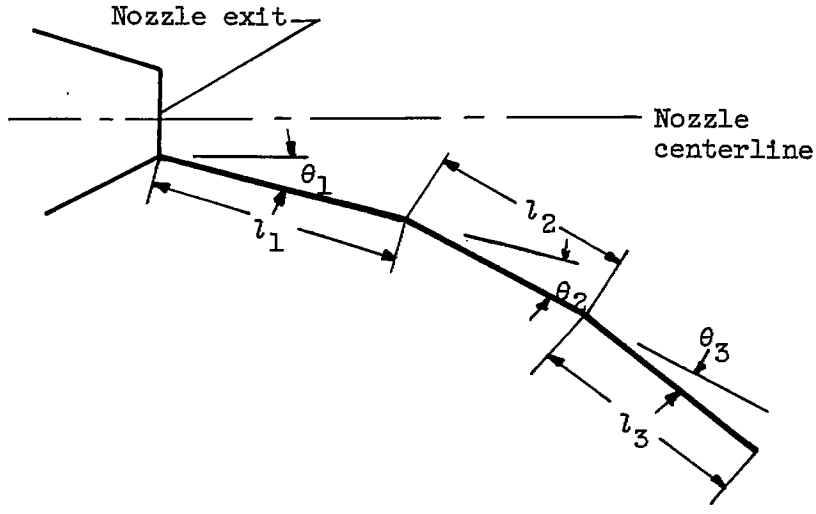

The total deflection-plate angle is

$$\theta_t = \theta_1 + \theta_2 + \theta_3$$

and the total deflection-plate length is

$$l_t = l_1 + l_2 + l_3$$

(All symbols are defined in appendix A.)

The deflection plate for six- and nine-flat-plate configurations consisted of a single piece of sheet metal bent at the appropriate downstream locations to yield the desired local deflection-plate length and angle. The juncture between the various plates consequently consisted of a curved radius section rather than the sharp-edged gap formed at the hinge line for the two- and three-flat-plate configurations. The six- and nine-flat-plate deflectors were attached to the nozzle by means of a piano hinge. A single telescoping tube supported the downstream end of the deflection plate in the same manner as in the previous configurations. For the nine-flat-plate configuration, the initial deflection-plate angle θ_1 could be varied $\pm 10^{\circ}$, thereby yielding some off-design performance data.

4807

Pertinent dimensions for all the multiple-flat-plate configurations studied are as follows:

Configuration, number of plates	Nozzle height, h, in.	Length of plate, in.			Deflection angle between adjacent plates, θ, deg
		l_1	l_2	l_3	
2	1.1	2.0 2.0	5.2 2.75	---- ----	Variable
3	1.1 0.5 and 2.0	2.0 2.5	2.75 2.75	4.88 4.88	Variable
6	2.0	l_1 to l_6, 2.0 each			12.5
9	0.5	l_1 to l_9, 0.6 each			10.0; θ_1 variable $\pm 10^{\circ}$

As in reference 2, side plates were attached to the deflection plates in order to delay jet-stream detachment from the plates. For the data presented herein, the side plates were equal in height to the nozzle height and were sealed to the jet-deflection plate to prevent air leakage. Limited data, not included herein, were obtained with side plates equal to twice the nozzle height and showed no difference from that obtained with side plates equal to the nozzle height. Pressure taps were located along the centerline of each jet-deflection plate for the two-, three-, and six-plate configurations. For the nine-flat-plate configuration, pressure taps were located on the odd-numbered plates.

Curved plates. - The curved-plate setup consisted of a box frame that was attached to the nozzle flange and supported a number of 1/8-inch aluminum plates stacked in the box at a 45° angle to the nozzle centerline (fig. 5). A template and jig were used to adjust these plates (which could be slid relative to each other) to the desired curved-plate profile. The deflection plate consisted of a sheet of spring brass (0.010 in. thick) sufficiently wide to adequately span the nozzle-exit width. In order to obtain surface pressure measurements, a plastic belt 1/16 inch thick and about 1 inch wide was cemented to the brass deflection plate at the centerline. To each side of this pressure belt, sheet rubber of thickness equal to the belt was cemented to the brass plate to provide a smooth, even surface. The upstream end of the finished deflection plate was secured to the nozzle by a special brass fitting machined to provide the proper jet-deflection angle from the nozzle exit to the deflection plate. The

deflection plate was then placed over the contoured stack of aluminum plates and anchored tightly in place by means of a cable and turnbuckle attached to the box frame and the downstream end of the deflection plate (fig. 5). Side plates of the same height as the nozzle and running the full length of the deflection plate were mounted on each side of the nozzle. The side plates were sealed to the plate to prevent air leakage onto or away from the deflection plate.

Sketches of the curved deflection-plate profiles studied (A to F) are shown in figure 6 together with pertinent dimensions. The curved plates consisted of a short straight section followed by a circular-arc section until a turning angle of 90° was obtained for the plate. Beyond the 90° angle, configurations A, B, C, and F were provided with an additional curved section.

PROCEDURE

Force and pressure data were obtained over a range of nominal pressure ratios across the nozzles from 1.5 to 3.0. The jet stream discharged into quiescent air at an ambient pressure of 29.2±0.3 inches of mercury. The forces on a Coanda nozzle and the moment arms are shown in the following sketch:

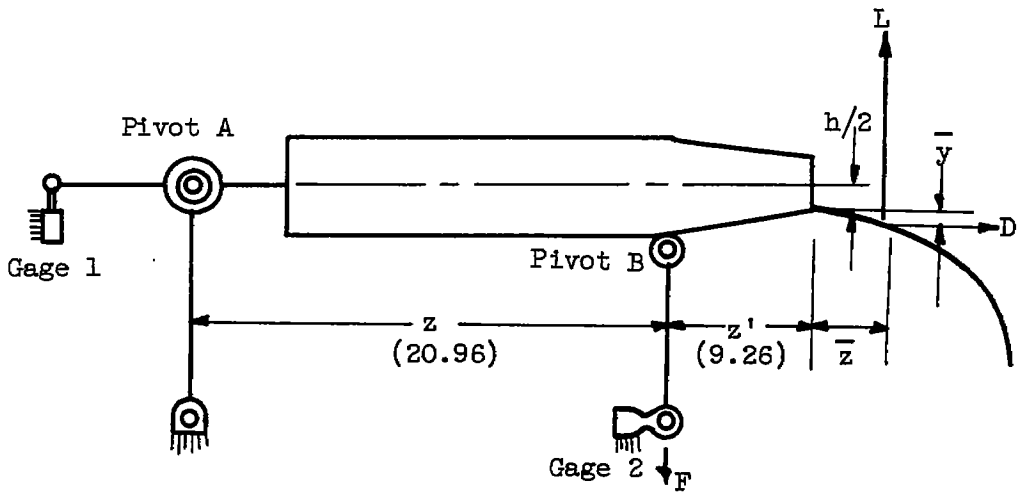

It was determined that the horizontal force measurements were independent of any vertical force; hence, the axial thrust was obtained directly from strain gage 1. The moment about pivot A consisted of two components, the lift caused by the deflection plate and the axial-thrust reduction (drag) caused by the plate. In calculating the net lift, moments about pivot A give the following equations:

$$L(z + z' + \bar{z}) + D\left(\frac{h}{2} + \bar{y}\right) = F(z) \tag{1}$$

or

$$L = \frac{F(20.96) - D\left(\frac{h}{2} + \bar{y}\right)}{(30.22 + \bar{z})} \tag{2}$$

The thrust-reduction force (drag of deflection plate) D was calculated by subtracting the measured axial thrust obtained with the deflected plate from that obtained with the undeflected jet (no deflection plate). The values of $\bar{y}$ and $\bar{z}$ were obtained from center-of-pressure calculations based on the pressure distribution over the deflection plate.

In general, the deflection plate for a particular Coanda nozzle was set at a predetermined angle and all pressure and force data were recorded as the nominal pressure ratio was increased progressively from 1.5 to 3.0. Data recording generally was terminated for any particular configuration when the jet stream became detached from the plate. Jet-stream detachment from the deflection plate was observed visually, since sufficient water vapor condensed out of the air leaving the nozzle to permit easy observation of the jet stream. At the time jet detachment was observed, lift force was reduced, axial thrust was increased to values approaching the undeflected thrust, and local surface pressures on the deflection plate approached the ambient pressure.

RESULTS AND DISCUSSION

General Considerations

The performance of each Coanda nozzle is evaluated in terms of the ratios of lift to undeflected thrust $\mathcal{F}_L$ and axial thrust to undeflected thrust $\mathcal{F}_z$, where the undeflected thrust is that obtained for each nozzle without a deflection plate. As a basis for comparison, the experimental $\mathcal{F}_L$ and $\mathcal{F}_z$ values obtained herein are compared with those obtained from a simplified theoretical analysis for a perfect curved-plate mechanical deflector (ref. 4) and with those obtained from an empirical relation for single- and multiple-flat-plate deflectors. The equations for the $\mathcal{F}_L$ and $\mathcal{F}_z$ values for the various flat-plate deflectors are described in appendix B and are summarized in the following table:

4807

Plate contour	Number of plates	Local angle between adjacent plates	$\mathscr{F}_L$	$\mathscr{F}_z$	Reference
Curved[a] (perfect)	1	--------	$\sin \theta_t$	$\cos \theta_t$	4
Flat	n	θ, variable	$\sum_{i=1}^{i=n} \tan \theta_i \cos \sum_{k=1}^{k=i} \theta_k$	$1 - \sum_{i=1}^{i=n} \tan \theta_i \sin \sum_{k=1}^{k=i} \theta_k$	Appendix B
Flat	1	θ_1	$\sin \theta_1$	$1 - \sin \theta_1 \tan \theta_1$	2 and appendix B

[a]Performance of this type deflector is said to follow the "cosine law."

As is evident from the table, the $\mathscr{F}_L$ and $\mathscr{F}_z$ values calculated by use of the applicable equations in appendix B for multiple-flat-plate configurations vary with the number of flat plates used and the local deflection angle between adjacent plates. In all cases the calculated $\mathscr{F}_L$ and $\mathscr{F}_z$ values for a multiple-flat-plate configuration are less than those for a perfect curved deflector. For a multiple-flat-plate deflector at total deflection angles beyond those obtainable with a single flat plate (ref. 2), decreasing $\mathscr{F}_L$ and $\mathscr{F}_z$ values are obtained with progressively fewer flat-plate segments. Conversely, as large numbers of flat-plate segments are used (constant total deflection angle), the surface contour approaches that of a curved surface, and $\mathscr{F}_L$ and $\mathscr{F}_z$ values near those given by the sine and cosine curve, respectively, are obtained. An example of the effect of the number of flat plates used to obtain a total jet-stream deflection of 60° on the calculated $\mathscr{F}_L$ and $\mathscr{F}_z$ values is shown in the following table, along with the values for the perfect curved plate:

Plate contour	Local angle between adjacent plates, deg	$\mathscr{F}_L$	$\mathscr{F}_z$
Two flat	30	0.789	0.211
Three flat	20	.803	.326
Six flat	10	.829	.420
Curved (cosine law)	θ_t, 60	.866	.500

The table shows a variation in the calculated $\mathscr{F}_L$ value based on that for a perfect curved plate of up to 9 percent, and in the calculated $\mathscr{F}_z$ value up to 58 percent depending on the deflection-plate contour.

Performance of Coanda Nozzles

The performance of the Coanda nozzles in terms of the ratio of lift to undeflected thrust $\mathscr{F}_L$ and ratio of axial to undeflected thrust $\mathscr{F}_z$ (hereinafter called axial-thrust ratio) as functions of total deflection-plate angle is presented in table I. Cross plots of these data show that the performance ($\mathscr{F}_L$ and $\mathscr{F}_z$) for a particular configuration at a given deflection angle is substantially independent of pressure ratio as long as jet detachment from the deflection plate does not occur. Consequently, the discussion of the data herein generally will be confined to a nominal pressure ratio of 2.1, and the trends of the data will be considered representative of those occurring at the other pressure ratios studied. Only performance data for no jet detachment from the deflection plates are discussed herein. Jet detachment usually occurred within 5° of the angles associated with the last data point given in table I.

The following general performance data were obtained with all configurations studied: (1) The experimental $\mathscr{F}_L$ and $\mathscr{F}_z$ values increased and decreased, respectively, with increasing total deflection-plate angle, and (2) the experimental $\mathscr{F}_L$ and $\mathscr{F}_z$ values were lower and higher, respectively, than calculated values. The departure of the experimental values from calculated values is attributed primarily to the facts that the jet stream was not turned the full deflection angle prescribed by the deflection plates and that the average jet total pressure decreased with increasing distance downstream of the nozzle exit (see appendixes C and D).

The following sections present details of the experimental over-all performance data for multiple-flat-plate and curved-plate Coanda nozzles in terms of $\mathscr{F}_L$ and $\mathscr{F}_z$ as functions of total deflection-plate angle θ_t. Also shown in the attendant figures are the applicable calculated $\mathscr{F}_L$ and $\mathscr{F}_z$ values for the particular configurations and, for comparative purposes, the curves obtained for single-flat-plate and perfect curved-plate mechanical deflectors. For convenience, the calculated $\mathscr{F}_L$ and $\mathscr{F}_z$ values for multiple-flat-plate configurations are shown by curves representing an average value at any θ_t for the particular combination of plates indicated by the experimental data points; the specific calculated values that apply for each configuration are within ± 2 percent of the average values given by the curves.

4807

CU-2

Two flat plates. - The $\mathscr{F}_L$ and $\mathscr{F}_z$ values for a Coanda nozzle using two flat plates to deflect the jet stream are shown in figure 7 as a function of θ_t. The data were obtained using a nozzle height of 1.1 inches and several plate lengths as noted in the figure. The measured $\mathscr{F}_L$ values are about 12 percent lower than the corresponding values calculated by use of appendix B. For the range of deflection angles shown in figure 7, the decrease in the calculated $\mathscr{F}_L$ values (estimated performance curve, fig. 7) from the sine curve amounts to about 3 percentage points. The measured $\mathscr{F}_z$ value at a θ_t of 50° falls about 54 percent above the calculated values. At small total deflection angles (less than 30°) the experimental $\mathscr{F}_z$ values fall approximately on the estimated performance curve.

At a particular total deflection-plate angle, greater $\mathscr{F}_L$ values usually are obtained for configurations with large θ_1 than with small θ_1. For example, at θ_t of 30° the configuration with θ_1 of 20° has an $\mathscr{F}_L$ value of 0.455 compared with $\mathscr{F}_L$ of 0.410 for a configuration with θ_1 of 10°. Within limits, the θ_2 at which jet detachment occurs from the deflection plate is independent of θ_1.

Because the local surface pressure coefficients were essentially zero over the last half of the second deflection plate (see appendix C), a reduction in the length of the second plate from 5.2 to 2.75 inches had no appreciable effect on the measured $\mathscr{F}_L$ and $\mathscr{F}_z$ values (fig. 7).

A comparison of the data shown in figure 7 with that given in reference 2 shows that a two-flat-plate configuration can be deflected to considerably larger θ_t values than a single flat plate before jet detachment occurs. Consequently, larger $\mathscr{F}_L$ values can be obtained with two flat plates than with a single flat plate. Specifically, for deflection-plate lengths and angles approaching optimum values (defined as deflectors having negative surface pressure coefficients over their entire surface with a zero pressure coefficient initially occurring at the downstream end of each plate; see also ref. 2), a two-flat-plate configuration can deflect the jet to angles about 50 percent greater and obtain $\mathscr{F}_L$ values about 30 percent larger than those obtainable with a single-flat-plate configuration.

Three flat plates. - The $\mathscr{F}_L$ and $\mathscr{F}_z$ values for Coanda nozzles using three flat plates to deflect the jet stream are shown in figure 8 as a function of θ_t. Nozzle heights of 2.0, 1.1, and 0.5 inch were used together with individual deflection-plate lengths of 2 to 4.88 inches as noted in the figure. In general, the data show the same trends of $\mathscr{F}_L$ and $\mathscr{F}_z$ with increasing θ_t and θ_1 values as discussed for the

two-flat-plate configurations. The reduction of the measured $\mathscr{F}_L$ values from those given by the estimated performance curve amounts to about 17 percent for θ_t values less than 60°. With a nozzle height of 0.5 inch (fig. 8(c)), it was possible to obtain total deflection-plate angles up to 89°; however, the attendant $\mathscr{F}_L$ values were only of the order of 0.66 (14 percent less than calculated values), because the lift was obtained primarily from the first two plates. The third plate, because of its steep deflection angle relative to the horizontal nozzle axis, contributed almost wholly to reducing the axial thrust.

The $\mathscr{F}_z$ values for θ_t near 60° (fig. 8(b)) are generally greater by up to 47 percent than those given by the estimated performance curve. At total deflection-plate angles near 90° (fig. 8(c)), the measured $\mathscr{F}_z$ value of 0.12 greatly exceeded the calculated value of -0.35 because of failure of the jet to turn the complete angle prescribed by the flat plates and because of the simplifying assumptions used in the equations presented in appendix B. The inability of the jet stream to turn the full total angle prescribed by the deflection plates was observed for all configurations and deflection angles; however, this phenomenon was more evident at large total deflection angles.

Six flat plates. - While the two- and three-flat-plate configurations were studied over arbitrarily selected deflection-plate lengths and angles, the individual plate lengths and angles for the six- and nine-flat-plate configurations (the latter to be discussed later) were calculated by use of the single-flat-plate data of reference 2 in order to obtain near optimum performance. For a prescribed total deflection-plate angle, equal local deflection angle between adjacent plates, and a given number of plates, a plate length was calculated that would result in negative surface pressure coefficients over the entire surface with a zero pressure coefficient approximately at the downstream end of each plate.

For the six-flat-plate Coanda nozzle ($h = 2.0$ in. and $\theta_t = 75°$), an $\mathscr{F}_L$ value of about 0.805 was attained compared with a calculated value of 0.896. The measured $\mathscr{F}_z$ value was 0.345 compared with the calculated value of 0.141, indicating that the jet stream did not turn the full 75° prescribed by the deflection plate. It is believed that the decrease in average total pressure of the jet stream with distance downstream from the nozzle exit also contributed to the reduced $\mathscr{F}_L$ and increased $\mathscr{F}_z$ values. Further discussion of the performance compared with that calculated empirically is contained in appendixes C and D.

A comparison of the $\mathscr{F}_L$ value obtained with the six-flat-plate configuration with that interpolated for the three-plate configuration at a θ_t of 75° (fig. 8(c)) shows that the $\mathscr{F}_L$ value for the six-plate configuration is about 19 percent greater than that for the three-plate configuration.

4807

CU-2 back

Nine flat plates. - The experimental and calculated $\mathscr{F}_L$ and $\mathscr{F}_z$ values for a nine-flat-plate Coanda nozzle (h = 0.5 in.) with each plate designed on the basis of optimum ratio of plate length to nozzle height for single plates (ref. 2) is shown in the following table. The data shown include the effect of using θ_1 values of 0°, 10°, and 20° with a corresponding change in θ_t of 80°, 90°, and 100°, respectively:

Local angle of first plate, θ_1, deg	Total deflection-plate angle, θ_t, deg	$\mathscr{F}_L$		$\mathscr{F}_z$	
		Exp.	Calc.	Exp.	Calc.
0	80	0.808	0.919	0.270	0.081
10	90	.885	.919	.135	-.096
20	100	.884	.892	.020	-----

A maximum $\mathscr{F}_L$ value of 0.885 was obtained at the design θ_t of 90°, compared with a calculated value of 0.919.

A change in θ_1 of ±10° from the design angle of 10° caused a deceease in the measured $\mathscr{F}_L$ values, especially when θ_1 was reduced to 0°. For θ_1 of 0°, the first plate contributed practically no lift, because, as shown in table I, the negative pressures (yielding lift) on this plate were balanced by positive pressure. Consequently, the $\mathscr{F}_L$ value was reduced (from 0.885 to 0.808), since the deflection plate consisted effectively of only eight plates with a θ_t of 80°. With a θ_1 of 20°, the lift on the first plate was increased; however, the last plate (θ_t = 100°) had a downward force component that decreased the lift gain from the first plate. Furthermore, the other plates (2 to 8) had somewhat reduced lift components because of flow interactions due to deflecting the first plate to a larger angle than that between the succeeding plates. The result of all of these effects caused the $\mathscr{F}_L$ value for θ_t of 100° to be substantially the same as that at θ_t of 90°.

For the three θ_t values studied with the nine-flat-plate configuration, the measured $\mathscr{F}_z$ values were always greater than those calculated. At a θ_t of 100°, however, the $\mathscr{F}_z$ was nearly zero, so that only vertical lift was being obtained.

4807

Curved plates. - Previous unpublished NACA data for Coanda nozzles have shown that, when a curved deflection plate is tangential to the nozzle centerline at the nozzle exit, a positive surface pressure relative to ambient pressure is obtained on the plate near the nozzle exit. This positive surface pressure causes a downward force on the plate and consequently reduces the over-all lift of the configuration. The curved plates used herein, therefore, consisted of a straight section inclined downward near the nozzle exit followed by the curved contours shown in figure 6. The straight section of the deflection plate was generally designed in accordance with optimum ratios of nozzle height to plate length presented in reference 2, with the result that only negative surface pressure coefficients occur on this portion of the deflection plate.

4807

The measured $\mathscr{F}_L$ and $\mathscr{F}_z$ values obtained with a Coanda nozzle using a curved deflection plate are summarized in the following table ($P_N/p_O = 2.1$):

Configuration	$\mathscr{F}_L$ values	$\mathscr{F}_z$ values[a]
A	0.815	-0.04
B	.810	-.02
C	.807	-.04
D	.770	.21
E	.803	.12
F	.803	-.02

[a]Minus signs indicate that the jet stream was turned more than 90°, yielding a reverse thrust in the axial direction; plus signs indicate that the jet stream was not turned 90°.

These data show that a curved surface with a 90° angle at the downstream end of the plate (configurations D and E) will not turn the jet stream as much as the deflection angle specified by the plate. It is necessary, therefore, to "overturn" the deflection plate (see configurations A, B, C, and F) by an angle of perhaps 10° in order to turn the jet stream the required 90° and obtain an $\mathscr{F}_z$ value of zero.

A comparison of the data obtained with the curved-plate configurations with those for the nine-flat-plate configuration shows that the latter has an $\mathscr{F}_L$ value about 0.07 higher than that of the curved plates (0.88 to 0.81, respectively). It should be noted, however, that the curved-plate configurations studied herein are not considered optimum deflection-plate profiles (see also appendix C). Also the details of the degree and

means for overturning the deflection plate at the downstream end have not been fully explored.

Comparison of Performance for all Coanda Nozzles Tested

The performance of the various Coanda nozzles studied herein is summarized in a plot of the variation of $\mathcal{F}_z$ with $\mathcal{F}_L$ shown in figure 9. The measured-data curves shown in figure 9 were obtained by fairing a curve through the highest $\mathcal{F}_L$ values at each θ_t presented in the previous figures and in the tables. Also shown in figure 9 are the performance curves for single-flat-plate and perfect curved-plate mechanical deflectors. All the data, except for the three-flat-plate configuration, used to deflect the jet near 90° (h = 0.5 in.), fall between the envelope of these two curves. The performance of the three-flat-plate configuration for a nozzle height of 0.5 inch was relatively poor, primarily because the $\mathcal{F}_L$ value was low since the third plate virtually did not contribute to lift, as discussed previously. The best performance (as defined by nearest approach of the experimental data to the cosine-law curve) for large total deflection-plate angles was obtained by the six- and nine-flat-plate configurations. In general, the measured $\mathcal{F}_L$ values of the best Coanda nozzles for θ_t values greater than 70° ($\mathcal{F}_z$ values less than about 0.3) were about 85 percent of those calculated for a perfect curved plate.

4807

CONCLUDING REMARKS

The results of this study show that Coanda nozzles using multiple-flat-plate or curved-plate deflectors can achieve a 90° deflection of the jet stream with vertical-lift values of the order of 0.88 and 0.81, respectively, of the undeflected thrust. These lift values are accompanied by an essentially zero axial-thrust component. The measured lift values are not considered to be optimum for a Coanda nozzle, higher values possibly being attainable with more refined deflectors.

For the Coanda nozzles used herein, side plates were required to delay jet-stream detachment from the deflection plate. The optimum shape and height for these side plates were not determined; however, side plates of the same height as the nozzle and extending the full length of the deflection plate appeared to be adequate.

As pointed out in reference 2, the deflection surfaces may necessarily be large in order to achieve good performance for a high degree of jet-stream turning for use with VTOL aircraft; therefore, best utilization of a Coanda nozzle can be achieved by designing an aircraft with due consideration of the unique characteristics of the device rather than by

incorporating it in an existing aircraft. Any trim or pitching moments that might be caused by the location of the center of pressure for the deflection plate (see table I) would have to be compensated for by an appropriate reaction control device.

4807

Lewis Flight Propulsion Laboratory
National Advisory Committee for Aeronautics
Cleveland, Ohio, July 24, 1958

APPENDIX A

SYMBOLS

D	deflection-plate drag force, lb
F	force measured by strain-gage system at location noted, lb
F_j	undeflected jet thrust (no deflection plate), lb
F_N	force or lift normal to plate surface, lb
$\mathscr{F}_L$	ratio of lift to undeflected thrust, L/F_j
$\mathscr{F}_z$	ratio of axial thrust with deflection plate to undeflected thrust (also called axial-thrust ratio)
h	nozzle height, in.
L	vertical lift, lb
l	length of an individual flat plate in a multiple-flat-plate configuration, in.
l_t	total length of deflection-plate configuration, in.
l'	surface distance measured from upstream end of a deflection plate to an arbitrary point on deflection plate, in.
P_j	jet total pressure, in. Hg gage
$P_{j,d}$	average total pressure of jet downstream of nozzle exit, in. Hg gage
$P_{j,m}$	maximum total pressure of jet downstream of nozzle exit, in. Hg gage
P_N	jet total pressure, in. Hg abs
p	local static pressure on deflection plate or in jet stream as noted, in. Hg abs
p_O	atmospheric pressure, in. Hg abs
$\bar{y}$	vertical location of center of pressure referenced to lower lip of nozzle exit, in.

$\bar{z}$ horizontal location of center of pressure referenced to nozzle-exit plane, in.

z,z' horizontal lever arms, in.

θ local deflection-plate angle, deg

θ_t total deflection-plate angle, deg

Subscripts:

L lift

1,2,3, ... plate number

4807

CU-3

APPENDIX B

ESTIMATED PERFORMANCE OF MULTIPLE-FLAT-PLATE DEFLECTORS

By Thomas F. Gelder

As demonstrated in reference 2, the experimental performance ($\mathscr{F}_L$ and $\mathscr{F}_Z$ values) of a single-flat-plate deflector is reasonably represented by the following expressions: 4807

$$\mathscr{F}_L = \sin \theta_1 \tag{B1a}$$

$$\mathscr{F}_Z = 1 - \tan \theta_1 \sin \theta_1 \tag{B2a}$$

from which, by definition,

$$L_1 = F_j \sin \theta_1 \tag{B1b}$$

$$D_1 = F_j \tan \theta_1 \sin \theta_1 \tag{B2b}$$

An integration of local pressure differences from ambient along the single-flat-plate length (plate area for unit width) can be represented by a single force normal to the plate $F_{N,1}$. The vertical (lift) and horizontal (drag) components of this normal force are

$$L_1 = F_{N,1} \cos \theta_1 \tag{B3}$$

and

$$D_1 = F_{N,1} \sin \theta_1 \tag{B4}$$

Combining (B3) and (B1b) or (B4) and (B2b) results in

$$F_{N,1} = F_j \tan \theta_1 \tag{B5}$$

By assuming that the jet stream will turn from the first plate and follow a second plate in the same manner (same losses and/or augmented flow) as it left the nozzle exit and followed the first plate, a method for predicting the performance of a two-plate deflector is suggested. Such reasoning implies a normal force on the second plate analogous to equation (B5), or

$$F_{N,2} = F_j \tan \theta_2 \tag{B6}$$

Likewise, throughout any given multiple-flat-plate deflectors,

$$F_{N,i} = F_j \tan \theta_i \tag{B7}$$

Since θ_i is defined as the local angle between adjacent plates, the lift and drag components of the ith plate are a generalization of equations (B3) and (B4), respectively, or

$$L_i = F_{N,i} \cos \sum_{i=1}^{i=n} \theta_i \tag{B8}$$

$$D_i = F_{N,i} \sin \sum_{i=1}^{i=n} \theta_i \tag{B9}$$

With equation (B7) the total lift and drag for a multiple-flat-plate configuration are, from (B8) and (B9),

$$\begin{aligned} L &= L_1 + L_2 + \dots L_n \\ &= F_j \left[\tan \theta_1 \cos \theta_1 + \tan \theta_2 \cos (\theta_1 + \theta_2) + \dots \sum_{i=1}^{i=n} \tan \theta_i \cos \sum_{k=1}^{k=i} \theta_k \right] \end{aligned} \tag{B10}$$

$$\begin{aligned} D &= D_1 + D_2 + \dots D_n \\ &= F_j \left[\tan \theta_1 \sin \theta_1 + \tan \theta_2 \sin (\theta_1 + \theta_2) + \dots \sum_{i=1}^{i=n} \tan \theta_i \sin \sum_{k=1}^{k=i} \theta_k \right] \end{aligned} \tag{B11}$$

From the definition of $\mathscr{F}_L$ and $\mathscr{F}_z$, equations (B10) and (B11) become

$$\begin{aligned} \mathscr{F}_L &= \frac{L}{F_j} \\ &= \tan \theta_1 \cos \theta_1 + \tan \theta_2 \cos (\theta_1 + \theta_2) + \dots \sum_{i=1}^{i=n} \tan \theta_i \cos \sum_{k=1}^{k=i} \theta_k \end{aligned} \tag{B12}$$

4807

CU-3 back

$$\mathscr{F}_z = \frac{F_j - D}{F_j}$$

$$= 1 - \left[\tan \theta_1 \sin \theta_1 + \tan \theta_2 \sin (\theta_1 + \theta_2) + \ldots \sum_{i=1}^{i=n} \tan \theta_i \sin \sum_{k=1}^{k=i} \theta_k\right] \tag{B13}$$

The performance estimates of multiple-flat-plate configurations using (B12) and (B13) represent maximum $\mathscr{F}_L$ and minimum $\mathscr{F}_z$ values to be expected and should only be used as a guide. Actual performance will depend on plate length, nozzle size, entrainment of surrounding air by the jet stream, and so forth, as discussed in reference 2, and also will differ from (B12) and (B13) because of losses in jet-stream total pressure as indicated in appendix D. Finally, local deflection angles are limited by jet-stream detachment from the deflection plate (ref. 2).

4807

APPENDIX C

PRESSURE DISTRIBUTION OVER DEFLECTION PLATES

Order of magnitude and trends of specific effects on the pressure distribution over the deflection plate due to pressure ratio, plate length, local and total deflection angles, number of plate segments, and nozzle height are discussed in this appendix.

A complete tabulation of the local surface pressure coefficients as a function of distance along the plate surface measured from the nozzle exit is given in table II for the multiple-flat-plate and curved-plate configurations.

Multiple Flat Plates

Representative pressure distributions for the multiple-flat-plate configurations are presented in figures 10 to 13 in terms of local surface pressure coefficient $(p - p_0)/P_j$ as a function of local deflection-plate length l' measured from the upstream end of each plate in the deflection-plate configuration. Pressure distributions for configurations having equal local deflection-plate angles $(\theta_1 = \theta_2 = \theta_3 \ldots)$ were selected for these figures. Furthermore, for each configuration the pressure distributions for the individual plates are superimposed for purposes of data comparison. Where possible, the pressure distribution for a single-flat-plate configuration (ref. 2) is also shown for comparison. Finally, small inserts in the figures show the local surface pressure coefficients as a function of the total deflection-plate length l_t.

The pressure-distribution trends observed for all multiple-flat-plate configurations are summarized as follows: The pressure distribution over the first plate of a multiple-flat-plate configuration has the same general shape as that for the single-flat-plate configuration (see figs. 10 to 12) except near the downstream end of the first plate, where the local surface pressure coefficient is greater for a multiple-flat-plate configuration than for the single-flat-plate configuration. A small decrease in $(p - p_0)/P_j$ near the upstream end of the plate also is evident for some of the multiple-flat-plate configurations. The second and succeeding plates of a multiple-flat-plate configuration show progressively decreasing local surface pressure coefficients (less negative values) near the upstream portions of the plate compared with the $(p - p_0)/P_j$ values for the first plate (and single-flat-plate data). The decrease in the local negative surface pressure coefficients over

the upstream portions of the second and succeeding deflection plates results in a decrease in lift for these plates compared with that predicted by single-flat-plate data. Some increase in lift is obtained by the higher negative $(p - p_0)/P_j$ values over the downstream portions of the first plate; however, the decrease in lift of the other plates in a configuration generally outweighs this improvement.

Details of the pressure distributions for each multiple-flat-plate configuration are discussed in the following sections.

4807

Two flat plates. - In figure 10(a) the pressure distribution over a two-flat-plate configuration is shown for nominal pressure ratios of 1.8 and 2.7 and a local deflection angle of 10° $(\theta_1 = \theta_2 = 10^{\circ})$. The dash-dot curve in the figure is the pressure distribution measured for an otherwise similar Coanda nozzle using a single-flat-plate deflector for θ_1 of 10° (ref. 2). Similar data at a local deflection angle of 20° and a P_N/p_0 of 2.7 are shown in figure 10(b). The general pressure-distribution trends described previously occur both for above and below nozzle choked-flow conditions. The decreased $\mathcal{F}_L$ value (compared with calculated) for the two-flat-plate configuration shown in figure 7 and discussed in the text is attributed primarily to the decrease in local surface pressure coefficients over the upstream portion of the second plate (square symbols, fig. 10).

It is of interest to note that the second plate for the configurations shown in figure 10 was excessively long, as evidenced by the initial location of the zero pressure coefficient upstream of the end of the plate (see ref. 2), and that some increase in $\mathcal{F}_L$ could be obtained by using a shorter second plate and thus deleting that portion of the plate over which positive pressures exist without affecting the remaining pressures over the rest of the plate (ref. 2).

Three flat plates. - The deviations of the pressure distribution for successive deflection plates of a three-flat-plate configuration compared with single-flat-plate data (fig. 11) followed the trends noted for the two-flat-plate configuration. The local surface pressure coefficients for the third plate (constant θ values) were lower (less negative) than those for either the first or second plate. This factor contributed largely to the decrease in $\mathcal{F}_L$ values for the three-flat-plate configurations (fig. 8) compared with calculated values.

Six flat plates. - The decrease in lift caused by the progressively reduced local surface pressure coefficients over successive plates of the six-flat-plate configuration (fig. 12) is illustrated by comparing the lift normal to the surface obtained from each plate (obtained by integration under the pressure-distribution curves) with that for the first

plate and that for a single flat plate (ref. 2). These comparisons in ratio form are shown in the following table:

Plate	Ratio of normal lift of each plate to normal lift of first plate	Ratio of normal lift of each plate to normal lift of single flat plate (ref. 2)
1	1.00	1.10
2	.69	.76
3	.64	.70
4	.60	.66
5	.56	.61
6	.25	.27

These data show that, except for the first and last plates, the plates contribute only about two-thirds of the normal lift obtainable with a single flat plate for the same operating conditions. The sixth plate has a normal lift only about one-fourth of that for the single flat plate. This low lift may be explained by the fact that the jet stream is not being turned to the complete θ_t of the deflection surface, and local jet detachment may be occurring.

Nine flat plates. - For the nine-flat-plate-configuration (fig. 13), the effect of decreased local surface pressure coefficients with downstream location of the particular deflection plate on the lift normal to each plate was substantially the same as for the six-flat-plate configuration. In the following table the lift normal to each instrumented plate (odd-numbered plates) is compared with that for the first plate:

Plate	Ratio of normal lift of each plate to normal lift of first plate
1	1.00
3	.91
5	.68
7	.57
9	.28

These data are for θ_t of 90° ($\theta_1 = 10^\circ$). As for the six-flat-plate configuration, the normal lift for the downstream plates is reduced.

Curved Plates

Typical pressure distributions over several curved-plate configurations are shown as a function of distance along the deflection plate in figure 14. In general, the local surface pressure coefficients over the straight section of the deflection plate are comparable in magnitude to those obtained with the single-flat-plate configurations of reference 2. In the transition region where the straight section fairs into the curved portion of the deflection plate, the local surface pressure coefficients increase again to reach large negative values (up to about -0.5). Following this negative surface-pressure-coefficient peak, in the transition region the coefficients oscillate widely in a series of alternating peaks and valleys before tending to decrease monotonically with increasing surface distance along the plate.

4807

Efforts to eliminate the regions of low negative pressure coefficients by a change in over-all radius of curvature of the deflection plate proved unsuccessful. It is believed that small local changes in curvature of the deflection plate would eliminate these valleys in the pressure distribution and thereby increase the lift obtainable with a curved deflection plate over the $\mathcal{F}_L$ values given in the text. The present setup, however, was not sufficiently flexible for the study of such local effects on the performance of the configuration.

The effect of pressure ratio on the pressure distribution over configuration A is shown in figure 14(a). It is apparent from these data that no systematic trends are discernible.

Pressure distributions for configurations E and F were substantially similar to those shown in figure 14 and are not further discussed.

APPENDIX D

EFFECT OF JET-STREAM TOTAL-PRESSURE LOSSES ON DEFLECTION-PLATE PRESSURE DISTRIBUTION AND LIFT CAPABILITY

The local pressures obtained on the surface of the deflection plates are expressed herein in terms of the average total pressure of the jet stream measured near the nozzle exit. Also, in the calculated performance herein it was assumed that the total pressure of the jet stream remains constant with distance downstream of the nozzle exit. However, for an undeflected jet, increasing total-pressure losses do occur with progressively increasing distance downstream of the nozzle exit because of mixing with the quiescent air surrounding the jet stream.

Total- and static-pressure traverses of the undeflected jet stream at several downstream stations were made with the 2-inch nozzle; the resultant total-pressure profiles are shown in figure 15(a) for a nominal pressure ratio of 2.1. It is apparent that the total-pressure profile increases in height (measured vertically from the nozzle centerline) and also that the maximum total pressure at the jet centerline decreases with increasing distance downstream of the nozzle exit. Near the nozzle exit (0.5 in. downstream) the total-pressure profile shows a nearly flat, rectangular shape similar to the shape usually existing at the nozzle exit. Farther downstream the total-pressure profile is no longer flat but shows a decrease in total pressure with increasing height measured vertically from the jet centerline.

These total-pressure profiles were integrated, and the ratio of the average total pressure downstream of the nozzle exit to total pressure at the nozzle exit $P_{j,d}/P_j$ is shown in figure 15(b) as a function of distance downstream of the nozzle exit for a range of pressure ratios. Figure 15(b) shows that the average total-pressure ratio $P_{j,d}/P_j$ decreases with increasing distance downstream of the nozzle exit. For the nozzle studied, $P_{j,d}/P_j$ of 0.56 was obtained 11.88 inches downstream of the nozzle exit. Also shown in figure 15(b) is the ratio of the maximum value (nozzle centerline) of the local jet total pressure to the total pressure at the nozzle exit $P_{j,m}/P_j$. This total-pressure ratio also decreases with distance from the nozzle exit, attaining a value of 0.66 11.88 inches downstream of the nozzle exit.

The deterioration of the jet total pressure downstream of the nozzle exit helps to explain in part the reduction in the local negative surface pressure coefficients on successive plates with a multiple-flat-plate configuration. All other factors remaining equal, the pressure distribution over each plate (hence normal lift) is a function of the total

pressure of the jet stream passing over each plate. A reduction in jet total pressure will therefore result in decreased local pressures on a plate and a reduction in normal lift over the surface. It was observed that, when the ratio of the average surface pressure coefficient for a given plate to that for a single flat plate is plotted as a function of distance downstream of the nozzle exit to the midchord of the particular plate, the resulting values are similar to those for the average total-pressure ratio $P_{j,d}/P_j$ given in figure 15(b). However, this observation may be fortuitous, since the effect of a deflector such as the six-flat-plate configuration on the local jet-stream total pressures was not determined. While an effort was made to obtain total-pressure profiles of the jet stream over the six-flat-plate deflector, the presence of the pressure probe markedly affected the pressure distribution over the plate being studied and caused a loss in lift for the configuration (in some cases jet separation from the deflector occurred). The total-pressure data obtained under these circumstances were not considered valid and therefore are not included herein.

4807

REFERENCES

1. Metral, Albert R.: Method of Increasing Fluid Stream by Diverting It from Its Axis of Flow. Coanda Effect. Trans. Rep. No. F-TS-823-Re, WADC-AMC, Feb. 1948.

2. Glahn, von, Uwe H.: Use of the Coanda Effect for Obtaining Jet Deflection and Lift with a Single Flat-Plate Deflection Surface. NACA TN 4272, 1958.

3. Glahn, von, Uwe H., and Povolny, John H.: Considerations of Some Jet-Deflection Principles for Directional Control and for Lift. Preprint No. 219, SAE, 1957.

4. McArdle, Jack G.: Internal Characteristics and Performance of Several Jet Deflectors at Primary-Nozzle Pressure Ratios up to 3.0. NACA TN 4264, 1958.

4807

CU-4 back

TABLE I. - SUMMARY OF PERFORMANCE CHARACTERISTICS

(a) Two-flat-plate configurations; nozzle height, 1.1 inches; l_1 = 2.0 inches

Deflection-plate angle, deg θ_1	θ_2	Pressure ratio, P_N/p_0	Ratio of lift to undeflected thrust, $\mathcal{F}_L$	Axial-thrust ratio, $\mathcal{F}_z$	$\bar{y}$, in.	$\bar{z}$, in.	Comments
l_2 = 5.2 in.							
10	10	1.51	0.301	0.929	-0.56	-0.23	
		1.82	.292	.909	.25	.75	
		2.11	.286	.894	.69	2.05	
		2.72	.304	.911	.17	1.26	
		3.04	.300	.899	.06	.96	
	15	1.51	0.329	0.881	0.67	1.60	
		1.82	.354	.860	.61	1.58	
		2.10	.356	.853	.84	2.12	
		3.05	.392	.836	.62	1.86	
	20	1.53	0.400	0.842	1.47	2.29	
		1.84	.413	.814	1.41	2.75	
		2.11	.413	.797	1.31	2.37	
		2.69	.427	.817	1.11	2.34	
		3.03	.447	.790	1.43	3.25	
	25	1.51	0.476	0.728	1.92	3.24	
		1.80	.480	.711	2.20	3.72	
		2.15	.496	.674	2.42	4.27	
		2.74	.498	.703	1.89	3.16	Jet detachment at $P_N/p_0 > 2.9$
	30	1.51	0.550	0.654	2.40	3.36	
		1.85	.526	.630	2.80	3.92	Jet detachment at $P_N/p_0 > 2.0$
15	10	1.50	0.369	0.878	0.36	1.00	
		1.80	.372	.871	.37	1.07	
		2.14	.373	.853	.38	1.18	
		2.71	.396	.870	.45	1.37	
		3.03	.397	.859	.34	1.31	
	20	1.52	0.491	0.786	1.02	1.58	
		1.83	.492	.758	1.22	1.51	
		2.10	.480	.744	1.33	1.97	
		2.72	.513	.762	1.01	1.86	
		3.00	.513	.754	1.69	2.70	
	25	1.52	0.531	0.699	1.75	2.11	
		1.83	.541	.672	2.12	2.64	
		2.14	.555	.625	2.42	3.05	
		2.70	.555	.691	1.83	2.45	
		3.06	.462	.734	2.57	3.13	Partial jet detachment
		2.87	.560	.672	2.32	2.99	
	30	1.50	0.589	0.597	2.44	2.66	
		1.82	.578	.570	2.71	2.95	
		2.70	.525	.682	2.74	2.80	
		3.04	.258	.891	2.09	1.79	Partial jet detachment
20	10	1.52	0.427	0.824	0.38	0.90	
		1.84	.442	.785	.44	1.01	
		2.14	.460	.813	.43	.91	
		3.06	.463	.805	.33	1.66	
	20	1.82	0.543	0.717	1.03	1.44	
		2.12	.552	.709	1.14	1.44	
		2.72	.556	.718	1.25	1.71	
		3.04	.493	.734	1.61	2.13	
	25	1.50	0.604	0.667	1.39	1.44	
		1.80	.600	.630	1.49	1.73	
		2.13	.600	.620	1.95	2.00	
		2.71	.588	.658	1.92	2.10	
		3.04	.492	.686	2.36	2.15	
	30	1.50	0.634	0.560	2.10	1.87	
		1.84	.635	.530	2.55	2.25	
		2.14	.586	.580	2.75	2.27	
		2.70	.569	.595	2.71	2.34	Jet detachment at $P_N/p_0 > 2.6$
l_2 = 2.75 in.							
15	10	1.51	0.377	0.913	0.36	0.96	
		1.83	.370	.893	.46	1.04	
		2.14	.375	.866	.48	1.08	
	20	1.53	0.490	0.811	1.14	1.34	
		1.83	.488	.763	1.41	1.92	
		2.13	.491	.751	1.35	2.03	
		2.75	.531	.744	1.33	2.02	
20	10	1.52	0.451	0.873	0.45	0.96	
		1.80	.455	.842	.50	1.13	
		2.12	.450	.827	.45	.95	
		2.68	.459	.822	.64	1.28	
		3.02	.442	.806	.87	1.61	
	15	1.50	0.505	0.811	0.59	1.06	
		1.82	.548	.782	.78	1.30	
		2.71	.517	.771	.91	1.51	
		3.05	.469	.773	1.27	2.02	
	20	1.50	0.562	0.785	0.95	1.37	
		1.83	.552	.736	1.19	1.59	
		2.11	.559	.702	1.38	1.64	
		2.58	.564	.705	1.47	1.91	
		3.03	.274	.859	1.09	1.36	Partial jet detachment

TABLE I. - Continued. SUMMARY OF PERFORMANCE CHARACTERISTICS

(b) Three-flat-plate configurations; l_2 = 2.75 inches; l_3 = 4.88 inches

Deflection-plate angle, deg			Pressure ratio, P_N/p_0	Ratio of lift to undeflected thrust, $\mathcal{F}_L$	Axial-thrust ratio, $\mathcal{F}_z$	$\bar{y}$, in.	$\bar{z}$, in.
θ_1	θ_2	θ_3					
h = 2.0 in.; l_1 = 2.5 in.							
10	10	20	1.51	0.498	0.723	3.88	5.48
			1.81	.492	.733	3.98	5.86
			2.12	.492	.712	4.17	6.50
			2.69	.548	.731	3.85	5.94
		15	1.51	0.478	0.813	2.98	4.56
			1.81	.465	.795	2.82	4.84
			2.13	.462	.704	3.03	4.96
			2.70	.497	.787	3.00	5.53
	15	20	1.52	0.556	0.711	3.88	5.01
			1.80	.526	.679	3.94	5.55
			2.13	.558	.667	3.80	5.36
			2.72	.543	.684	4.01	5.82
15	15	20	1.50	0.608	0.644	4.08	4.04
			1.81	.593	.634	4.20	4.15
			2.11	.613	.616	4.32	4.03
			2.70	.578	.647	3.93	4.62
h = 1.1 in.; l_1 = 2.0 in.							
10	10	10	----	-----	-----	----	----
			2.08	0.399	0.841	2.73	3.02
			2.72	.423	.838	1.97	3.59
			2.96	.434	.808	2.22	3.37
		20	1.82	0.465	0.743	3.88	5.07
			2.09	.477	.721	3.51	4.74
			2.66	.504	.717	2.64	4.89
			3.00	.476	.716	3.90	5.38
		25	1.83	0.488	0.676	4.70	5.79
			2.12	.504	.639	4.76	5.78
			2.69	.507	.653	5.18	6.05
			3.01	.487	.678	5.03	5.62
15	20	25	1.81	0.637	0.482	4.38	3.29
			2.10	.633	.469	4.49	3.39
			2.68	.643	.474	4.46	3.33
			2.98	.623	.539	4.24	3.55
20	10	10	1.80	0.532	0.730	1.36	1.91
			2.10	.535	.726	1.51	1.98
			2.67	.549	.730	1.91	2.36
			2.98	.523	.741	1.90	2.50
		20	1.83	0.604	0.612	3.31	2.81
			2.12	.602	.606	3.56	2.93
			2.70	.568	.617	3.46	2.95
			3.00	.542	.665	3.40	3.12
	20	10	1.80	0.618	0.612	2.21	2.13
			2.12	.631	.600	2.25	2.13
			2.72	.633	.642	2.28	2.22
			3.04	.532	.691	1.85	2.19
		20	1.80	0.688	0.484	3.57	2.40
			2.11	.679	.477	3.59	2.44
			2.69	.658	.535	3.52	2.47
			3.01	.559	.663	2.39	2.38
h = 0.5 in.; l_1 = 2.5 in.							
20	25	25	1.80	0.682	0.316	3.78	2.60
			2.10	.665	.270	3.65	2.84
			2.72	.654	.285	3.88	2.90
			3.03	.672	.273	4.21	2.53
22	25	30	1.80	0.689	0.236	4.37	2.20
			2.10	.683	.198	4.29	2.29
			2.69	.648	.180	4.86	2.60
25	26	33	1.80	0.683	0.137	4.96	1.65
			2.11	.642	.106	5.08	1.91
			2.70	.638	.068	5.23	1.91
			3.03	.630	.046	5.79	1.87
	32	32	1.80	0.693	0.068	4.32	1.66
			2.12	.658	.061	4.60	1.93
			2.70	.674	.033	4.51	1.99
			3.02	.673	.018	4.68	2.10

4807

TABLE I. - Concluded. SUMMARY OF PERFORMANCE CHARACTERISTICS

(c) Six-flat-plate configuration; nozzle height, 2.0 inches; each deflection-plate angle, $12\frac{1}{2}^{\circ}$; each plate length, 2.0 inches

Pressure ratio, P_N/p_0	Ratio of lift to undeflected thrust, $\mathcal{F}_L$	Axial-thrust ratio, $\mathcal{F}_z$	$\bar{y}$, in.	$\bar{z}$, in.
1.50	0.785	0.315	[a]5.2	[a]3.4
1.78	.788	.318	[a]5.2	[a]3.4
2.12	.808	.345	5.23	3.4

[a]Estimated.

(d) Nine-flat-plate configurations; nozzle height, 0.5 inch; each plate length, 0.6 inch; deflection-plate angles θ_2 to θ_9, 10° each

θ_1, deg	Pressure ratio, P_N/p_0	Ratio of lift to undeflected thrust, $\mathcal{F}_L$	Axial-thrust ratio, $\mathcal{F}_z$	$\bar{y}$, in. (a)	$\bar{z}$, in. (a)
0	1.79	0.811	0.277	2.25	1.5
	2.10	.808	.270	2.25	1.6
	2.71	.835	.253	2.0	1.7
10	1.82	0.880	0.135	2.0	1.4
	2.10	.885	.135	2.0	1.4
	2.71	.885	.135	1.9	1.6
	3.00	.885	.130	1.8	1.8
20	1.81	0.873	0	2.0	1.3
	2.11	.884	.020	2.0	1.3
	2.69	.873	.014	1.8	1.5
	3.02	.861	0	1.8	1.65

[a]Estimated.

(e) Curved-plate configurations; nozzle height, 1.1 inches

Configuration	Plate length, in.	Pressure ratio, P_N/p_0	Ratio of lift to undeflected thrust, $\mathcal{F}_L$	Axial-thrust ratio, $\mathcal{F}_z$ (a)	$\bar{y}$, in.	$\bar{z}$, in.
A	8.25	1.49	0.800	0.	2.25	2.08
		1.80	.819	-.03	2.24	1.86
		2.09	.815	-.04	2.27	2.02
		2.46	.810	0	2.15	2.06
		2.66	.766	.19	1.95	2.01
B	9.00	1.49	0.801	0.02	2.70	2.10
		1.81	.804	0	2.69	2.15
		2.11	.810	-.02	2.65	2.10
		2.69	.788	.10	2.39	2.42
		2.88	.774	.01	2.27	2.56
C	7.60	1.79	0.842	-0.03	2.23	1.60
		2.09	.807	-.04	2.22	1.63
D	11.25	2.09	0.770	0.21	[b]3.2	[b]4.5
E	11.25	2.09	0.803	0.12	[b]2.95	[b]4.5
F	8.25	2.11	0.803	-0.02	[b]2.0	[b]2.3

[a]Negative sign indicates reverse thrust (excessive turning of jet stream).

[b]Estimated.

TABLE II. - PRESSURE DISTRIBUTIONS FOR MULTIPLE-FLAT-PLATE AND CURVED-PLATE COANDA NOZZLES

(a) Two-flat-plate configuration; nozzle height, 1.1 inches; length of first plate, 2.0 inches

(1) l_2 = 5.2 in.; p_0 = 28.93 in. Hg abs; θ_1 = 10°

Plate angle	θ_2, 10°					θ_2, 15°					θ_2, 20°					θ_2, 25°				θ_2, 30°	
P_N/p_0	1.51	1.82	2.11	2.72	3.04	1.51	1.82	2.10	2.71	3.05	1.53	1.84	2.11	2.69	3.03	1.51	1.80	2.15	2.74	1.51	1.85
P_j, in. Hg gage	14.80	23.85	32.15	49.70	58.95	14.80	23.70	31.85	49.60	59.25	15.35	24.30	32.10	48.80	58.60	14.90	23.30	33.20	50.30	14.70	24.70
Local surface distance, in.	Local surface pressure coefficient, $(p - p_0)/P_j$																				
$l_1' = 0.25$	-0.28	-0.33	-0.38	-0.15	-0.08	-0.34	-0.32	-0.34	-0.12	-0.04	-0.38	-0.34	-0.34	-0.12	-0.04	-0.33	-0.31	-0.30	-0.10	-0.35	-0.34
.50	-.17	-.23	-.29	-.09	-.02	-.27	-.20	-.27	-.07	-0	-.28	-.21	-.27	-.08	0	-.25	-.20	-.23	-.06	-.27	-.19
.75	-.07	-.14	-.25	-.12	-.06	-.15	-.11	-.22	-.11	-.04	-.17	-.11	-.22	-.11	-.04	-.15	-.10	-.26	-.09	-.16	-.08
1.0	-.03	-.06	-.02	-.19	-.12	-.06	-.04	-0	-.17	-.11	-.07	-.04	-.10	-.18	-.11	-.05	-.03	-.01	-.16	-.08	-.02
1.25	-.03	-.02	.05	-.27	-.20	-.03	-.01	.07	-.25	-.19	-.03	-.01	.06	-.25	-.19	-.01	0	.08	-.24	-.02	<.01
1.50	-.07	<-.01	.07	-.31	-.25	-.03	-0	.07	-.30	-.24	-.03	0	.07	-.31	-.24	-.01	.01	.08	-.30	-.01	.01
1.75	-.10	-.04	.03	-.15	-.29	-.09	-.03	.03	-.15	-.28	-.08	-.03	.03	-.11	-.29	-.05	.01	.04	-.10	-.05	-.02
$l_2' = 0.5$	-0.02	-0.12	-0.36	-0.09	-0.19	-0.22	-0.24	-0.39	-0.22	-0.25	-0.32	-0.28	-0.26	-0.29	-0.21	-0.27	-0.22	-0.18	-0.33	-0.25	-0.19
1.0	-0	-.01	-0	-.08	-.10	-.07	-.08	-.14	-.20	-.18	-.18	-.22	-.21	-.25	-.19	-.25	-.21	-.19	-.17	-.26	-.19
1.5	.01	.01	.05	-.02	-.02	-.02	-.01	-.04	-.06	-.10	-.08	-.15	-.16	-.12	-.16	-.23	-.21	-.19	-.14	-.25	-.20
2.0	.01	.01	.03	.09	.08	0	.01	.02	.03	-.03	-.02	-.09	-.10	-.04	-.13	-.19	-.20	-.19	-.12	-.08	-.20
2.5	.01	.01	.02	.01	.07	.01	.01	.03	.02	.02	.01	-.03	-.03	.01	-.09	-.14	-.18	-.19	-.10	-.22	-.20
3.0	.01	.01	.01	-.02	-.03	.01	.01	.03	.08	<.01	.02	.01	-.02	.06	-.04	-.07	-.14	-.17	-.08	-.16	-.19
3.5	.01	.01	.01	.04	.02	.01	.01	.02	.01	.08	.02	.03	.04	.04	-0	-.02	-.09	-.14	-.05	-.07	-.17
4.0	<.01	.01	.01	.02	.05	.01	.01	.01	-.01	.05	.01	.03	.03	.04	.03	.02	-.02	-.08	-.02	-.01	-.11
4.5	<.01	<.01	<.01	<-.01	.04	0	0	<.01	.02	-.03	.01	.02	.02	<.01	.03	.03	.02	-.03	.01	.03	-.04

(2) l_2 = 5.2 in.; p_0 = 28.93 in. Hg abs; θ_1 = 15°

Plate angle	θ_2, 25°					θ_2, 35°					θ_2, 40°					θ_2, 45°				
P_N/p_0	1.50	1.80	2.14	2.71	3.03	1.52	1.83	2.10	2.72	3.00	1.52	1.83	2.14	2.70	3.06	1.50	1.82	2.15	2.70	3.04
P_j, in. Hg gage	14.40	23.10	32.90	49.60	58.60	15.15	24.15	31.85	49.80	57.90	15.20	24.00	33.10	49.30	59.55	14.50	23.75	33.25	49.30	-0.02
Local surface distance, in.	Local surface pressure coefficient, $(p - p_0)/P_j$																			
$l_1' = 0.25$	-0.42	-0.37	-0.45	-0.22	-0.14	-0.42	-0.37	-0.46	-0.21	-0.14	-0.41	-0.36	-0.43	-0.20	-0.13	-0.42	-0.36	-0.44	-0.21	-0.16
.50	-.40	-.35	-.39	-.18	-.11	-.39	-.34	-.39	-.17	-.10	-.38	-.33	-.37	-.16	-.09	-.39	-.33	-.38	-.17	-.12
.75	-.32	-.29	-.24	-.20	-.13	-.32	-.28	-.22	-.19	-.13	-.31	-.27	-.26	-.18	-.12	-.31	-.27	-.28	-.19	-.14
1.0	-.23	-.22	-.16	-.24	-.17	-.22	-.20	-.14	-.23	-.17	-.21	-.19	-.13	-.23	-.16	-.21	-.20	-.15	-.24	-.18
1.25	-.14	-.16	-.10	-.30	-.23	-.14	-.12	-.07	-.29	-.23	-.12	-.12	-.06	-.29	-.23	-.13	-.13	-.08	-.30	-.22
1.50	-.08	-.10	-.02	-.32	-.28	-.09	-.09	<-.01	-.34	-.28	-.08	-.08	.01	-.34	-.27	-.08	-.08	-.01	-.19	-.06
1.75	-.07	-.08	<-.01	-.18	-.31	-.10	-.08	<.01	-.29	-.32	-.09	-.07	.02	-.26	-.11	-.08	-.07	.01	-.13	-.03
$l_2' = 0.5$	-0.08	-0.09	-0.22	-0.10	-0.19	-0.25	-0.24	-0.27	-0.23	-0.21	-0.30	-0.25	-0.21	-0.21	-0.08	-0.29	-0.20	-0.10	-0.09	-0.02
1.0	-.05	-.03	<.01	-.09	-.12	-.13	-.16	-.16	-.18	-.21	-.22	-.21	-.20	-.18	-.08	-.26	-.20	-.10	-.10	-.02
1.5	-.01	-.01	.01	.02	-.04	-.06	-.10	-.10	-.09	-.14	-.16	-.18	-.19	-.16	-.09	-.23	-.19	-.10	-.10	-.02
2.0	<.01	-0	.01	.05	.05	-.02	-.05	-.05	-.02	-.11	-.10	-.14	-.17	-.13	-.09	-.20	-.18	-.11	-.11	-.03
2.5	.01	.01	.01	-.01	.06	0	-.02	-.01	<.01	-.07	-.05	-.11	-.15	-.08	-.09	-.16	-.17	-.11	-.10	-.03
3.0	<.01	<.01	.01	.01	-.01	.01	<.01	.01	.04	-.04	-.02	-.07	-.13	-.03	-.08	-.11	-.15	-.10	-.10	-.03
3.5	<.01	<.01	.01	.04	0	.01	.01	.02	.01	<-.01	0	-.03	-.09	<-.01	-.08	-.07	-.12	-.09	-.09	-.03
4.0	0	<.01	<.01	-.01	.06	<.01	.01	.02	.03	.02	.01	<-.01	-.05	.01	-.07	-.02	-.09	-.08	-.08	-.02
4.5	<-.01	0	<.01	-.02	.02	<.01	.01	.01	.01	.01	.01	.01	-.01	.02	-.06	.01	-.05	-.05	-.06	-.02

TABLE II. - Continued. PRESSURE DISTRIBUTIONS FOR MULTIPLE-FLAT-PLATE AND CURVED-PLATE COANDA NOZZLES

(a) Concluded. Two-flat-plate configuration; nozzle height, 1.1 inches; length of first plate, 2.0 inches

(3) l_2 = 5.2 in.; p_0 = 28.83 in. Hg abs; θ_1 = 20°

Plate angle	θ_2, 10°					θ_2, 20°					θ_2, 25°					θ_2, 30°			
P_N/p_0	1.52	1.84	2.14	2.71	3.05	1.49	1.82	2.12	2.72	3.04	1.50	1.80	2.13	2.71	3.04	1.50	1.84	2.14	2.70
P_j, in. Hg gage	15.00	24.35	33.10	48.50	59.50	14.30	23.60	32.45	49.70	59.00	14.45	23.15	32.80	48.35	59.00	14.55	24.30	33.05	49.25
Local surface distance, in.	Local surface pressure coefficient, $(p - p_0)/P_j$																		
l_1 = 0.25	-0.37	-0.33	-0.47	-0.31	-0.22	-0.43	-0.39	-0.53	-0.30	-0.22	-0.44	-0.40	-0.52	-0.30	-0.22	-0.43	-0.38	-0.52	-0.30
.50	-.39	-.34	-.37	-.27	-.18	-.43	-.40	-.38	-.28	-.19	-.44	-.40	-.39	-.28	-.18	-.44	-.38	-.38	-.26
.75	-.38	-.34	-.31	-.28	-.20	-.42	-.37	-.31	-.27	-.21	-.42	-.38	-.30	-.28	-.20	-.41	-.38	-.30	-.27
1.0	-.38	-.31	-.28	-.30	-.23	-.38	-.34	-.27	-.30	-.23	-.38	-.34	-.27	-.30	-.23	-.38	-.32	-.28	-.30
1.25	-.30	-.28	-.24	-.34	-.27	-.32	-.30	-.21	-.34	-.27	-.32	-.30	-.21	-.35	-.27	-.30	-.28	-.21	-.34
1.5	-.24	-.24	-.15	-.21	-.30	-.25	-.25	-.14	-.38	-.31	-.26	-.24	-.13	-.26	-.30	-.23	-.23	-.13	-.19
1.75	-.17	-.19	-.09	-.17	-.20	-.20	-.20	-.10	-.24	-.22	-.21	-.20	-.08	-.21	-.16	-.18	-.18	-.08	-.15
l_2 = 0.5	-0.08	-0.10	-0.09	-0.12	-0.16	-0.18	-0.19	-0.21	-0.19	-0.17	-0.24	-0.23	-0.23	-0.18	-0.13	-0.28	-0.23	-0.14	-0.13
1.0	-.03	-.05	-.03	-.08	-.12	-.10	-.13	-.15	-.15	-.16	-.15	-.17	-.18	-.17	-.14	-.23	-.20	-.14	-.14
1.5	<-.01	-.01	-.01	-.02	-.05	-.05	-.08	-.10	-.10	-.12	-.09	-.13	-.16	-.14	-.14	-.18	-.18	-.13	-.14
2.0	.01	.01	<.01	.01	.01	-.01	-.04	-.05	-.04	-.08	-.05	-.09	-.12	-.10	-.13	-.14	-.16	-.13	-.14
2.5	.01	.01	.01	.01	.03	<.01	-.01	-.01	-.01	-.04	-.01	-.05	-.09	-.07	-.11	-.10	-.13	-.12	-.13
3.0	.01	.01	.01	.02	<-.01	.01	.01	.01	.01	-.01	0	-.02	-.05	-.04	-.08	-.05	-.10	-.11	-.12
3.5	.01	.01	.01	-.01	.02	.01	.01	.02	.01	.01	.01	<.01	-.02	-.02	-.04	-.02	-.07	-.10	-.10
4.0	<.01	.01	<.01	.01	.02	.01	.01	.02	.01	.01	.01	.01	0	0	-.01	0	-.04	-.08	-.08
4.5	0	<.01	0	<.01	-.03	<.01	.01	.01	0	.01	.01	.01	.01	<.01	.02	.01	-.01	-.06	-.03

(4) l_2 = 2.75 in.; p_0 = 29.80 in. Hg abs

Plate angle	θ_1, 15°; θ_2, 10°				θ_1, 15°; θ_2, 20°				θ_1, 20°; θ_2, 10°					θ_1, 20°; θ_2, 15°					θ_1, 20°; θ_2, 20°				
P_N/p_0	1.51	1.85	2.14	2.72	1.53	1.83	2.13	2.75	1.52	1.80	2.12	2.88	3.02	1.50	1.82	2.12	2.71	3.05	1.50	1.83	2.11	2.58	3.05
P_j, in. Hg gage	14.80	24.00	32.85	49.60	15.25	24.05	32.55	50.50	14.90	23.05	32.40	48.45	58.35	14.40	23.80	32.30	49.40	59.20	14.45	23.95	32.10	45.75	58.70
Local surface distance, in.	Local surface pressure coefficient, $(p - p_0)/P_j$																						
l_1 = 0.25	-0.42	-0.38	-0.45	-0.22	-0.43	-0.38	-0.48	-0.20	-0.38	-0.34	-0.49	-0.32	-0.23	-0.41	-0.38	-0.50	-0.31	-0.22	-0.43	-0.39	-0.50	-0.34	-0.24
.50	-.43	-.35	-.39	-.18	-.40	-.35	-.39	-.16	-.39	-.36	-.38	-.29	-.20	-.42	-.39	-.38	-.27	-.19	-.44	-.40	-.38	-.31	-.21
.75	-.32	-.29	-.25	-.20	-.32	-.30	-.24	-.19	-.38	-.35	-.32	-.30	-.22	-.41	-.37	-.32	-.28	-.21	-.42	-.37	-.31	-.32	-.22
1.0	-.22	-.21	-.16	-.25	-.22	-.20	-.14	-.23	-.38	-.33	-.29	-.32	-.24	-.37	-.33	-.29	-.31	-.23	-.37	-.33	-.27	-.34	-.24
1.25	-.14	-.15	-.07	-.31	-.14	-.14	-.07	-.29	-.32	-.29	-.24	-.36	-.28	-.32	-.29	-.23	-.38	-.27	-.31	-.29	-.21	-.38	-.09
1.50	-.08	-.10	-.02	-.33	-.10	-.09	<-.01	-.35	-.26	-.25	-.16	-.21	-.32	-.25	-.24	-.14	-.29	-.31	-.25	-.24	-.14	-.23	-.06
1.75	-.07	-.08	<-.01	-.18	-.11	-.09	<.01	-.33	-.18	-.20	-.10	-.17	-.19	-.18	-.19	-.11	-.22	-.21	-.19	-.20	-.10	-.17	-.04
l_2 = 0.5	-0.08	-0.08	-0.21	-0.11	-0.29	-0.25	-0.28	-0.23	-0.08	-0.10	-0.08	-0.12	-0.15	-0.05	-0.14	-0.16	-0.16	-0.17	-0.19	-0.19	-0.21	-0.19	-0.03
1.0	-.02	-.03	<.01	-.08	-.12	-.16	-.17	-.18	-.02	-.04	-.03	-.07	-.11	-.08	-.08	-.07	-.11	-.15	-.11	-.13	-.15	-.16	-.03
1.5	<-.01	<-.01	.02	.03	-.06	-.10	-.10	-.10	0	-.01	<-.01	-.01	-.05	-.02	-.04	-.03	-.04	-.09	-.06	-.08	-.09	-.12	-.03
2.0	<.01	<.01	.02	.04	-.02	-.05	-.04	-.03	.01	.01	.01	.01	.01	0	-.01	<-.01	-.01	-.03	-.02	-.04	-.05	-.07	-.03
2.5	.01	<.01	.01	-.01	<-.01	-.01	-.01	-.02	.01	.01	.01	.01	.02	.01	.01	<.01	-0	0	<-.01	-.01	-.01	-.02	-.04

TABLE II. - Continued. PRESSURE DISTRIBUTIONS FOR MULTIPLE-FLAT-PLATE AND CURVED-PLATE COANDA NOZZLES

(b) Three-flat-plate configuration; l_2, 2.75 inches; l_3, 4.88 inches

(1) h = 2.0 in.; l_1 = 2.5 in.; p_0 = 28.96 in. Hg abs

Plate angle	θ_1, 10°; θ_2, 10°; θ_3, 15°				θ_1, 10°; θ_2, 10°; θ_3, 20°				θ_1, 10°; θ_2, 15°; θ_3, 20°				θ_1, 15°; θ_2, 15°; θ_3, 20°			
p_N/p_0	1.51	1.81	2.13	2.70	1.51	1.81	2.12	2.69	1.52	1.80	2.13	2.72	1.50	1.81	2.11	2.70
P_j, in. Hg gage	14.75	23.55	32.80	49.35	14.70	23.40	32.55	49.10	15.05	23.30	32.65	49.95	14.60	23.35	32.20	49.35
Local surface distance, in.	Local surface pressure coefficient, $(p - p_0)/P_j$															
l_1' = 0.25	-0.48	-0.63	-0.36	-0.13	-0.49	-0.64	-0.36	-0.13	-0.49	-0.64	-0.35	-0.11	-0.58	-0.78	-0.49	-0.23
.50	-.38	-.45	-.27	-.05	-.38	-.42	-.27	-.04	-.38	-.39	-.26	-.03	-.54	-.64	-.42	-.17
.75	-.29	-.20	-.26	-.05	-.29	-.18	-.26	-.04	-.29	-.15	-.26	-.03	-.49	-.42	-.41	-.16
1.0	-.21	-.07	-.30	-.10	-.20	-.06	-.30	-.09	-.20	-.06	-.30	-.08	-.43	-.27	-.44	-.19
1.25	-.15	-.03	-.36	-.17	-.14	-.02	-.32	-.17	-.14	-.02	-.34	-.16	-.36	-.20	-.48	-.24
1.50	-.11	-.01	-.16	-.24	-.10	-.01	-.11	-.23	-.11	-.01	-.10	-.23	-.30	-.15	-.38	-.29
1.75	-.10	-.01	-.04	-.24	-.09	-.01	.01	-.22	-.10	-.01	.01	-.23	-.24	-.11	-.25	-.33
2.0	-.11	-.02	.05	-.21	-.10	-.03	.07	-.20	-.11	-.02	.08	-.20	-.22	-.09	-.16	-.28
l_2' = 0.5	-0.24	-0.52	-0.32	-0.31	-0.24	-0.50	-0.34	-0.31	-0.42	-0.65	-0.46	-0.37	-0.30	-0.46	-0.35	-0.38
1.0	-.15	-.13	-.35	-.24	-.15	-.12	-.37	-.23	-.30	-.30	-.49	-.36	-.22	-.21	-.35	-.33
1.5	-.12	-.05	-.19	-.18	-.12	-.05	-.16	-.19	-.19	-.18	-.33	-.24	-.17	-.13	-.13	-.26
2.0	-.11	-.05	.03	-.22	-.11	-.05	.02	-.22	-.16	-.12	-.14	-.31	-.16	-.11	-.05	-.21
2.5	-.18	-.10	.01	-.19	-.19	-.10	<.01	-.19	-.20	-.14	-.07	-.29	-.21	-.14	-.07	-.18
l_3' = 0.45	-0.26	-0.27	-0.42	-0.16	-0.34	-0.30	-0.51	-0.25	-0.28	-0.27	-0.35	-0.20	-0.29	-0.25	-0.25	-0.18
.95	-.16	-.15	-.25	-.12	-.24	-.23	-.25	-.20	-.21	-.20	-.19	-.18	-.22	-.20	-.21	-.15
1.45	-.11	-.10	-.08	-.14	-.18	-.18	-.17	-.18	-.16	-.15	-.14	-.15	-.16	-.16	-.18	-.13
1.95	-.07	-.07	-.04	-.11	-.14	-.15	-.13	-.12	-.13	-.12	-.11	-.13	-.13	-.13	-.15	-.11
2.45	-.05	-.04	-.02	-.04	-.11	-.12	-.10	-.09	-.10	-.10	-.09	-.10	-.10	-.11	-.12	-.09
2.95	-.03	-.03	-.01	-.01	-.07	-.10	-.07	-.07	-.08	-.08	-.06	-.07	-.08	-.09	-.10	-.06
3.45	-.02	-.01	~0	-.01	-.05	-.07	-.05	-.05	-.06	-.06	-.04	-.05	-.05	-.07	-.07	-.04
3.95	-.02	-.01	0	-.03	-.03	-.04	-.03	-.03	-.04	-.04	-.02	-.03	-.03	-.04	-.05	-.02
4.45	-.01	~0	<.01	-.02	-.02	-.02	-.01	-.01	-.02	-.02	-.01	-.01	-.02	-.03	-.03	-.01

4807

CU-5

TABLE II. - Continued. PRESSURE DISTRIBUTIONS FOR MULTIPLE-FLAT-PLATE AND CURVED-PLATE COANDA NOZZLES

(b) Continued. Three-flat-plate configuration; l_2, 2.75 inches; l_3, 4.88 inches

(2) h = 1.1 in.; l_1 = 2.0 in.; p_0 = 29.25 in. Hg abs

Plate angle	θ_1, 10°; θ_2, 10°; θ_3, 10°			θ_1, 10°; θ_2, 10°; θ_3, 20°				θ_1, 10°; θ_2, 10°; θ_3, 25°				θ_1, 15°; θ_2, 20°; θ_3, 25°			
P_N/p_0	2.08	2.72	2.96	1.82	2.09	2.66	3.00	1.83	2.12	2.69	3.01	1.81	2.10	2.68	2.98
P_j, in. Hg gage	31.75	50.40	57.25	24.05	32.00	48.55	58.45	24.40	32.80	49.45	58.70	23.60	32.25	49.25	57.85
Local surface distance, in.	Local surface pressure coefficient, $(p - p_0)/P_j$														
$l_1' = 0.25$	-0.36	-0.12	-0.06	-0.33	-0.44	-0.13	-0.04	-0.34	-0.32	-0.11	-0.03	-0.37	-0.46	-0.22	-0.14
.50	-.29	-.08	-.02	-.19	-.27	-.06	-0	-.18	-.25	-.07	<.01	-.35	-.38	-.17	-.10
.75	-.17	-.12	-.06	-.10	-.19	-.12	-.05	-.08	-.25	-.11	-.04	-.29	-.21	-.20	-.13
1.0	<-.01	-.18	-.12	-.04	.01	-.19	-.11	-.02	<.01	-.17	-.11	-.21	-.15	-.24	-.18
1.25	.06	-.25	-.20	-.01	.07	-.26	-.19	<-.01	.08	-.25	-.19	-.14	-.07	-.30	-.23
1.5	.06	-.31	-.26	-.01	.06	-.29	-.25	-0	.07	-.31	-.24	-.10	-0	-.33	-.28
1.75	.02	-.15	-.30	-.05	.02	-.10	-.29	-.04	.03	-.13	-.29	-.09	.01	-.23	-.32
$l_2' = 0.5$	-0.32	-0.09	-0.17	-0.11	-0.35	-0.08	-0.18	-0.11	-0.35	-0.10	-0.18	-0.26	-0.31	-0.23	-0.27
1.0	.01	-.09	-.10	-.01	<.01	-.14	-.11	-.01	-.01	-.10	-.11	-.16	-.18	-.20	-.21
1.5	.03	.01	-.01	-0	.04	.02	-.01	<.01	.04	.01	-.01	-.10	-.10	-.11	-.15
2.0	.02	.10	.10	-0	.02	.10	.09	0	.03	.10	.09	-.07	-.05	-.04	-.11
2.5	-.02	-.01	.05	-.05	-.02	-.02	.06	-.05	-.02	-.01	-.06	-.09	-.06	-.05	-.07
$l_3' = 0.45$	-0.23	-0.21	-0.23	-0.26	-0.24	-0.34	-0.27	-0.24	-0.21	-0.15	-0.13	-0.22	-0.21	-0.21	-0.13
.95	<-.01	-.21	-.18	-.19	-.18	-.16	-.18	-.22	-.20	-.15	-.13	-.16	-.16	-.15	-.11
1.45	-.01	.01	-.04	-.12	-.12	-.12	-.15	-.19	-.19	-.15	-.13	-.12	-.13	-.11	-.09
1.95	-.01	.05	.09	-.06	-.07	-.09	-.10	-.15	-.17	-.15	-.13	-.09	-.09	-.09	-.08
2.45	-.01	.01	.02	-.02	-.03	-.06	-.06	-.10	-.14	-.14	-.12	-.06	-.06	-.06	-.06
2.95	0	.04	-.01	-0	<-.01	-.02	-.03	-.05	-.10	-.12	-.11	-.03	-.04	-.04	-.05
3.45	<.01	.03	.06	.01	.01	<.01	<-.01	-.01	-.05	-.10	-.09	-.02	-.02	-.03	-.03
3.95	0	.03	-.02	<.01	.01	.01	.01	.01	-.01	-.07	-.07	-.01	<-.01	-.01	-.02
4.45	-0	<.01	-.01	-0	.01	.01	.01	.01	.01	-.03	-.04	-0	-0	.01	<-.01

Plate angle	θ_1, 20°; θ_2, 10°; θ_3, 10°				θ_1, 20°; θ_2, 10°; θ_3, 20°				θ_1, 20°; θ_2, 20°; θ_3, 10°				θ_1, 20°; θ_2, 20°; θ_3, 20°			
P_N/p_0	1.80	2.10	2.67	2.98	1.83	2.12	2.70	3.00	1.80	2.12	2.72	3.04	1.80	2.11	2.69	3.01
P_j, in. Hg gage	23.40	32.10	48.75	57.95	24.40	32.75	49.85	58.65	23.35	32.85	50.40	59.75	23.55	32.45	49.35	58.85
Local surface distance, in.	Local surface pressure coefficient, $(p - p_0)/P_j$															
$l_1' = 0.25$	-0.33	-0.47	-0.32	-0.24	-0.35	-0.53	-0.31	-0.23	-0.40	-0.54	-0.30	-0.22	-0.41	-0.54	-0.31	-0.23
.50	-.35	-.37	-.29	-.20	-.36	-.39	-.27	-.20	-.41	-.40	-.26	-.19	-.41	-.39	-.27	-.19
.75	-.34	-.32	-.30	-.23	-.35	-.31	-.29	-.22	-.38	-.31	-.27	-.21	-.38	-.31	-.28	-.21
1.0	-.32	-.28	-.32	-.25	-.32	-.28	-.31	-.24	-.34	-.28	-.30	-.23	-.34	-.27	-.31	-.24
1.25	-.29	-.22	-.36	-.29	-.28	-.22	-.35	-.29	-.30	-.21	-.34	-.27	-.29	-.20	-.35	-.28
1.5	-.25	-.15	-.20	-.32	-.24	-.14	-.21	-.31	-.25	-.13	-.38	-.31	-.24	-.12	-.38	-.31
1.75	-.20	-.11	-.16	-.19	-.19	-.10	-.17	-.19	-.20	-.10	-.27	-.25	-.20	-.09	-.25	-.27
$l_2' = 0.5$	-0.09	-0.08	-0.12	-0.15	-0.10	-0.08	-0.12	-0.16	-0.20	-0.24	-0.21	-0.19	-0.21	-0.24	-0.20	-0.20
1.0	-.04	-.03	-.07	-.11	-.05	-.03	-.07	-.11	-.14	-.15	-.15	-.18	-.12	-.15	-.16	-.18
1.5	-.01	-.01	-.01	-.04	-.02	-.01	-.01	-.04	-.09	-.10	-.09	-.13	-.10	-.10	-.10	-.12
2.0	<-.01	<-.01	<.01	-.02	-.02	<.01	.01	.02	-.06	-.06	-.04	-.08	-.07	-.06	-.05	-.07
2.5	-.04	-.04	<-.01	.01	-.07	-.04	-.02	.01	-.06	-.05	-.05	-.04	-.10	-.08	-.06	-.05
$l_3' = 0.45$	-0.07	-0.10	-0.16	-0.17	-0.22	-0.24	-0.29	-0.16	-0.07	-0.07	-0.06	-0.02	-0.18	-0.18	-0.15	-0.05
.95	-.03	-.03	-.11	-.03	-.12	-.15	-.14	-.10	-.04	-.04	-.04	-.01	-.11	-.11	-.08	-.03
1.45	-.01	-.01	.02	.02	-.07	-.09	-.08	-.07	-.02	-.02	-.01	-.01	-.07	-.07	-.05	-.02
1.95	-0	-0	.01	.01	-.03	-.05	-.04	-.04	-.01	-.01	-.01	0	-.04	-.04	-.04	-.01
2.45	-0	<.01	.01	-.01	-.01	-.03	-.01	-.03	-.01	<-.01	<-.01	<.01	-.02	-.02	-.03	<-.01
2.95	0	0	-0	.01	-.01	-.01	<-.01	-.02	-.01	-0	-.01	-0	-.01	-.01	-.02	<-.01
3.45	<.01	<.01	.01	-0	-0	-0	0	-.01	-0	-0	-0	<.01	-.01	<-.01	-.01	-0
3.95	0	0	0	-.01	0	0	-0	<-.01	-0	0	<-.01	-0	<-.01	<-.01	-.01	-0
4.45	-0	-0	-0	.01	0	-0	0	-0	0	-0	-0	-0	-0	0	-.01	-0

TABLE II. - Continued. PRESSURE DISTRIBUTIONS FOR MULTIPLE-FLAT-PLATE AND CURVED-PLATE COANDA NOZZLES

(b) Concluded. Three-flat-plate configuration; l_2, 2.75 inches; l_3, 4.88 inches

(3) h = 0.5 in.; l_1 = 2.5 in.; p_0 = 29.25 in. Hg abs

Plate angle	θ_1, 20°; θ_2, 25°; θ_3, 25°				θ_1, 22°; θ_2, 25°; θ_3, 30°			θ_1, 25°; θ_2, 26°; θ_3, 33°				θ_1, 25°; θ_2, 32°; θ_3, 32°			
P_N/p_0	1.80	2.10	2.72	3.03	1.80	2.10	2.69	1.80	2.11	2.70	3.03	1.80	2.12	2.70	3.02
P_j, in. Hg gage	23.50	32.15	50.30	59.25	23.30	32.15	49.40	23.55	32.55	49.70	59.30	23.30	32.70	49.70	59.00
Local surface distance, in.	Local surface pressure coefficient, $(p - p_0)/P_j$														
l_1' = 0.25	-0.31	-0.47	-0.27	-0.19	-0.29	-0.43	-0.31	-0.27	-0.27	-0.35	-0.26	-0.26	-0.27	-0.35	-0.26
.50	-.21	-.20	-.28	-.21	-.26	-.21	-.32	-.25	-.24	-.34	-.28	-.25	-.24	-.33	-.28
.75	-.12	-.07	-.15	-.30	-.21	-.16	-.16	-.24	-.22	-.17	-.21	-.23	-.22	-.17	-.20
1.0	-.03	.02	-.13	-.13	-.14	-.09	-.13	-.20	-.18	-.15	-.16	-.20	-.18	-.15	-.16
1.25	.03	.05	-.06	-.12	-.06	-.03	-.07	-.16	-.13	-.12	-.14	-.16	-.13	-.12	-.14
1.50	.04	.04	.03	-.05	<.01	.02	-.01	-.11	-.08	-.08	-.10	-.11	-.08	-.08	-.10
1.75	.03	.03	.09	.02	.03	.04	.05	-.06	-.03	-.03	-.05	-.06	-.03	-.03	-.05
2.0	.03	.04	.06	.10	.04	.05	.06	-.01	.01	<.01	.01	-.02	.01	~0	.01
l_2' = 0.5	-0.24	-0.21	-0.18	-0.19	-0.22	-0.21	-0.18	-0.15	-0.19	-0.17	-0.16	-0.22	-0.22	-0.19	-0.19
1.0	-.16	-.19	-.17	-.14	-.10	-.16	-.15	-.06	-.10	-.13	-.10	-.12	-.17	-.18	-.17
1.5	-.04	-.10	-.13	-.07	-.02	-.06	-.09	-.02	-.03	-.06	-.03	-.05	-.11	-.14	-.13
2.0	.02	.01	-.06	-.02	.01	.01	-.01	-.01	-.01	-.01	<-.01	-.02	-.04	-.08	-.09
2.5	-.02	<-.01	-.01	-.01	-.04	-.02	-.01	-.05	-.04	-.02	-.02	-.05	-.03	-.04	-.05
l_3' = 0.45	-0.12	-0.12	-0.10	-0.12	-0.17	-0.16	-0.14	-0.17	-0.15	-0.14	-0.12	-0.15	-0.13	-0.11	-0.11
.95	-.04	-.04	-.05	-.07	-.08	-.09	-.10	-.12	-.11	-.11	-.11	-.09	-.07	-.07	-.08
1.45	-.01	-.01	-.02	-.04	-.03	-.04	-.06	-.07	-.07	-.08	-.10	-.05	-.04	-.04	-.05
1.95	<-.01	-.01	-.01	-.01	-.01	-.01	-.03	-.03	-.04	-.05	-.08	-.02	-.02	-.02	-.03
2.45	<-.01	<-.01	-.01	-.01	<-.01	<-.01	-.02	-.01	-.02	-.03	-.05	-.01	-.02	-.02	-.02
2.95	<-.01	<-.01	-.01	<-.01	~0	<-.01	~0	-.01	-.01	-.02	-.03	-.01	-.01	-.01	-.01
3.45	0	0	~0	~0	~0	~0	<-.01	<-.01	<-.01	-.01	-.02	<-.01	<-.01	-.01	-.01
3.95	<-.01	<-.01	<-.01	~0	~0	~0	<-.01	<-.01	<-.01	<-.01	-.01	<-.01	<-.01	<-.01	<-.01
4.45	0	0	0	0	~0	~0	~0	0	~0	~0	~0	~0	~0	~0	~0

4807

CU-5 back

TABLE II. - Continued. PRESSURE DISTRIBUTIONS FOR MULTIPLE-FLAT-PLATE AND CURVED-PLATE COANDA NOZZLES

(c) Six-flat-plate configuration; nozzle height, 2.0 inches; θ_1, θ_2, . . . θ_6, 12.5° each; l_1, l_2, . . . l_6, 2.0 inches each; p_0, 29.43 inches of mercury absolute

P_N/p_0	1.44	1.78	2.12	2.71	P_N/p_0	1.44	1.78	2.12	2.71
P_j, in. Hg gage	14.80	23.10	33.10	50.40	P_j, in. Hg gage	14.80	23.10	33.10	50.40
Local surface distance, in.	Local surface pressure coefficient, $(p - p_0)/P_j$				Local surface distance, in.	Local surface pressure coefficient, $(p - p_0)/P_j$			
$l_1' = 0.03$	-0.74	-0.90	-0.54	-0.21	$l_4' = 0.03$	-0.38	-0.38	-0.35	-0.21
.15	-.70	-.71	-.42	-.15	.15	-.30	-.30	-.32	-.20
.28	-.63	-.62	-.36	-.10	.28	-.26	-.25	-.30	-.19
.52	-.47	-.47	-.28	-.04	.52	-.22	-.20	-.26	-.18
.78	-.36	-.29	-.29	-.05	.78	-.20	-.18	-.21	-.16
1.03	-.29	-.15	-.36	-.13	1.03	-.19	-.18	-.16	-.16
1.53	-.26	-.13	-.40	-.26	1.53	-.21	-.19	-.14	-.17
1.94	-.45	-.42	-.39	-.38	1.94	-.35	-.34	-.28	-.23
$l_2' = 0.03$	-0.45	-0.63	-0.45	-0.45	$l_5' = 0.03$	-0.38	-0.38	-0.37	-0.31
.15	-.34	-.67	-.39	-.46	.15	-.28	-.29	-.32	-.30
.28	-.29	-.57	-.33	-.46	.28	-.24	-.25	-.28	-.26
.53	-.24	-.27	-.26	-.46	.52	-.20	-.19	-.22	-.20
.78	-.22	-.17	-.26	-.45	.78	-.17	-.17	-.18	-.16
1.03	-.22	-.15	-.24	-.43	1.03	-.17	-.15	-.15	-.14
1.53	-.24	-.19	-.16	-.32	1.53	-.18	-.17	-.15	-.14
1.94	-.38	-.37	-.19	-.31	1.94	-.29	-.29	-.27	-.23
$l_3' = 0.03$	-0.42	-0.49	-0.30	-0.38	$l_6' = 0.03$	-0.29	-0.30	-0.30	-0.28
.15	-.33	-.36	-.30	-.42	.15	-.21	-.22	-.22	-.21
.28	-.27	-.28	-.29	-.40	.28	-.17	-.17	-.18	-.18
.52	-.24	-.20	-.30	-.31	.52	-.13	-.12	-.12	-.13
.78	-.21	-.18	-.27	-.29	.78	-.10	-.09	-.09	-.10
1.03	-.20	-.17	-.21	-.28	1.03	-.07	-.07	-.07	-.07
1.53	-.23	-.20	-.13	-.25	1.53	-.03	-.03	-.04	-.04
1.94	-.38	-.38	-.28	-.22	1.94	-.01	-.02	-.01	-.01

(d) Nine-flat-plate configuration; nozzle height, 0.5 inch; θ_2, θ_3, . . . θ_9, 10° each; l_1, l_2, . . . l_9, 0.5 inch each; p_0, 29.25 inches of mercury absolute

Plate angle	θ_1, 0°			θ_1, 10°				θ_1, 20°			
P_N/p_0	1.79	2.10	2.71	1.82	2.10	2.71	3.00	1.81	2.11	2.69	3.02
P_j, in. Hg gage	23.10	32.20	49.85	24.00	32.10	50.00	58.55	23.85	32.45	49.40	59.15
Local surface distance, in.	Local surface pressure coefficient, $(p - p_0)/P_j$										
$l_1' = 0.03$	-0.10	-0.03	0.10	-0.60	-0.32	-0.06	-0.01	-0.62	-0.49	-0.24	-0.15
.16	.04	.11	.31	-.32	-.22	-.01	.07	-.52	-.46	-.23	-.15
.28	.04	.03	.18	-.22	-.23	-.01	.06	-.45	-.45	-.22	-.14
.42	<.01	-.01	.06	-.13	-.29	-.10	-.03	-.37	-.49	-.26	-.18
.55	-.10	<.01	-.05	-.14	-.33	-.20	-.13	-.31	-.41	-.33	-.24
$l_3' = 0.03$	0.01	0.14	-0.38	-0.39	-0.27	-0.31	-0.27	-0.26	-0.21	-0.31	-0.28
.16	.01	-.16	-.37	-.31	-.35	-.19	-.26	-.16	-.24	-.29	-.29
.28	-.08	-.15	-.38	-.09	-.34	-.14	-.25	-.11	-.10	-.25	-.29
.42	-.06	-.02	-.23	-.09	-.14	-.11	-.24	-.12	-.06	-.01	-.28
.55	-.17	-.07	-.19	-.18	-.06	-.07	-.23	-.20	-.13	-.18	-.26
$l_5' = 0.03$	-0.39	-0.23	-0.18	-0.37	-0.29	-0.26	-0.18	-0.32	-0.31	-0.21	-0.14
.16	-.15	-.28	-.17	-.16	-.33	-.18	-.16	-.16	-.26	-.16	-.13
.28	-.09	-.12	-.19	-.10	-.13	-.13	-.12	-.12	-.10	-.10	-.12
.42	-.09	-.04	-.19	-.11	-.05	-.10	-.09	-.13	-.08	-.08	-.12
.55	-.19	-.11	-.20	-.19	-.13	-.09	-.09	-.20	-.16	-.14	-.12
$l_7' = 0.03$	-0.22	-0.27	-0.11	-0.23	-0.28	-0.21	-0.18	-0.22	-0.27	-0.21	-0.18
.16	-.13	-.17	-.13	-.15	-.17	-.24	-.17	-.15	-.16	-.18	-.18
.28	-.09	-.08	-.11	-.11	-.10	-.16	-.14	-.12	-.11	-.11	-.14
.42	-.10	-.08	-.09	-.11	-.10	-.08	-.10	-.12	-.11	-.11	-.12
.55	-.16	-.15	-.13	-.17	-.17	-.10	-.11	-.17	-.18	-.15	-.13
$l_9' = 0.03$	-0.14	-0.19	-0.18	-0.15	-0.18	-0.19	-0.16	-0.15	-0.16	-0.15	-0.11
.16	-.08	-.10	-.13	-.09	-.10	-.10	-.10	-.08	-.09	-.09	-.06
.28	-.05	-.05	-.06	-.05	-.05	-.05	-.05	-.05	-.05	-.04	-.04
.42	-.04	-.04	-.03	-.04	-.04	-.03	-.03	-.04	-.04	-.03	-.02
.55	-.04	-.04	-.03	-.04	-.04	-.03	-.02	-.03	-.03	-.02	-.02

TABLE II. - Concluded. PRESSURE DISTRIBUTIONS FOR MULTIPLE-FLAT-PLATE AND CURVED-PLATE COANDA NOZZLES

(e) Curved-plate configurations; nozzle height, 0.5 inch

Configuration	A				B				C		D				E				F			
p_0, in. Hg abs	29.13				29.07				29.38		29.45				29.45				29.09			
P_N/p_0	1.49	1.82	2.09	2.66	1.49	1.81	2.11	2.69	1.79	2.09	1.79	2.09	2.70	2.99	1.52	1.82	2.09	2.71	1.50	1.80	2.11	2.44
P_j, in. Hg gage	14.30	23.85	31.80	48.30	14.30	23.45	32.30	49.25	23.30	32.15	23.30	32.10	50.20	58.50	15.25	24.20	32.15	50.45	14.70	23.35	32.40	41.90
Local surface distance, l', in.	Local surface pressure coefficient, $(p - p_0)/P_j$																					
0.25	-0.57	-0.65	-0.43	-0.19	-0.24	-0.23	-0.12	0.06	-0.54	-0.31	-0.46	-0.24	-0.03	0.02	-0.36	-0.49	-0.30	-0.08	-0.36	-0.49	-0.29	-0.15
.31	-.49	-.61	-.40	-.18	-.22	-.17	-.10	.07	-.48	-.27	-.33	-.17	.04	.09	-.26	-.36	-.19	-0	-.27	-.35	-.30	-.16
.44	-.33	-.63	-.42	-.20	-.28	-.14	-.13	.05	-.45	-.27	-.23	-.18	.03	.10	-.21	-.38	-.22	-.03	-.16	-.17	-.18	-.04
.56	-.18	-.45	-.29	-.07	-.45	-.23	-.28	-.05	-.41	-.27	-.08	-.25	-.02	.06	-.20	-.44	-.26	-.03	-.08	-.08	-.10	.09
.69	-.14	-.25	-.35	-.12	-.44	-.32	-.37	-.18	-.45	-.35	-.03	-.30	-.05	.02	-.20	-.43	-.34	-.08	-.06	-.01	-.16	-.02
.94	-.13	-.04	-.48	-.24	-.34	-.45	-.47	-.32	-.31	-.55	-.04	-.29	-.15	-.09	-.21	-.09	-.46	-.20	-.15	-.08	-.29	-.21
1.19	-.14	-.03	-.17	-.33	-.29	-.49	-.45	-.39	-.23	-.57	-.12	-.03	-.27	-.21	-.16	-.08	-.25	-.29	-.21	-.19	-.26	-.38
1.44	-.17	-.08	-.10	-.40	-.29	-.45	-.39	-.43	-.22	-.46	-.13	.02	-.34	-.29	-.18	-.13	-.15	-.39	-.27	-.25	-.04	-.39
1.69	-.23	-.18	-.05	-.45	-.28	-.20	-.44	-.46	-.36	-.31	-.16	-.06	-.36	-.35	-.18	-.16	-.06	-.40	-.33	-.32	-.15	-.40
2.19	-.34	-.34	-.18	-.30	-.27	-.23	-.33	-.45	-.39	-.18	-.20	-.19	-.19	-.35	-.19	-.20	-.07	-.30	-.32	-.37	-.35	-.31
2.69	-.32	-.38	-.38	-.29	-.26	-.22	-.07	-.37	-.31	-.32	-.17	-.27	-.16	-.25	-.19	-.22	-.23	-.31	-.32	-.24	-.45	-.38
3.19	-.36	-.30	-.44	-.33	-.28	-.27	-.23	-.31	-.34	-.38	-.18	-.22	-.14	-.31	-.20	-.21	-.25	-.19	-.36	-.37	-.36	-.32
3.69	-.33	-.33	-.28	-.21	-.25	-.21	-.29	-.23	-.38	-.36	-.16	-.07	-.17	-.17	-.22	-.19	-.27	-.09	-.30	-.25	-.15	-.32
4.19	-.35	-.32	-.20	-.23	-.24	-.23	-.18	-.22	-.25	-.26	-.16	-.17	.01	-.09	-.17	-.17	-.08	-.01	-.31	-.29	-.25	-.20
4.69	-.29	-.25	-.33	-.24	-.22	-.20	-.22	-.18	-.28	-.23	-.15	-.16	-.07	-.02	-.17	-.16	-.17	-.13	-.30	-.27	-.35	-.21
5.19	-.27	-.25	-.30	-.23	-.23	-.21	-.19	-.04	-.28	-.31	-.16	-.15	-.19	-.14	-.16	-.15	-.12	-.14	-.29	-.27	-.32	-.34
5.69	-.28	-.27	-.21	-.14	-.24	-.22	-.22	-.18	-.28	-.21	-.14	-.14	-.25	-.14	-.18	-.17	-.15	-.15	-.27	-.24	-.19	-.30
6.19	-.24	-.23	-.26	-.12	-.23	-.22	-.24	-.31	-.20	-.18	-.15	-.15	-.23	-.17	-.18	-.18	-.20	-.19	-.24	-.22	-.29	-.23
7.19	-.16	-.15	-.15	-.08	-.20	-.19	-.19	-.10	-.13	-.11	-.16	-.14	-.06	-.17	-.16	-.15	-.15	-.21	-.13	-.12	-.11	-.11
8.19	-.11	-.10	-.07	-.04	-.11	-.11	-.10	-.03	-----	-----	-.14	-.14	-.17	-.16	-.15	-.14	-.14	-.08	-.10	-.10	-.07	-.04
9.19	-----	-----	-----	-----	-----	-----	-----	-----	-----	-----	-.13	-.13	-.13	-.10	-.14	-.14	-.15	-.17	-.03	<-.01	0	0
10.2	-----	-----	-----	-----	-----	-----	-----	-----	-----	-----	-.12	-.12	-.14	-.16	-.09	-.10	-.11	-.12	-----	-----	-----	-----
11.2	-----	-----	-----	-----	-----	-----	-----	-----	-----	-----	-.06	-.06	-.05	-.04	-.06	-.07	-.06	-.05	-----	-----	-----	-----

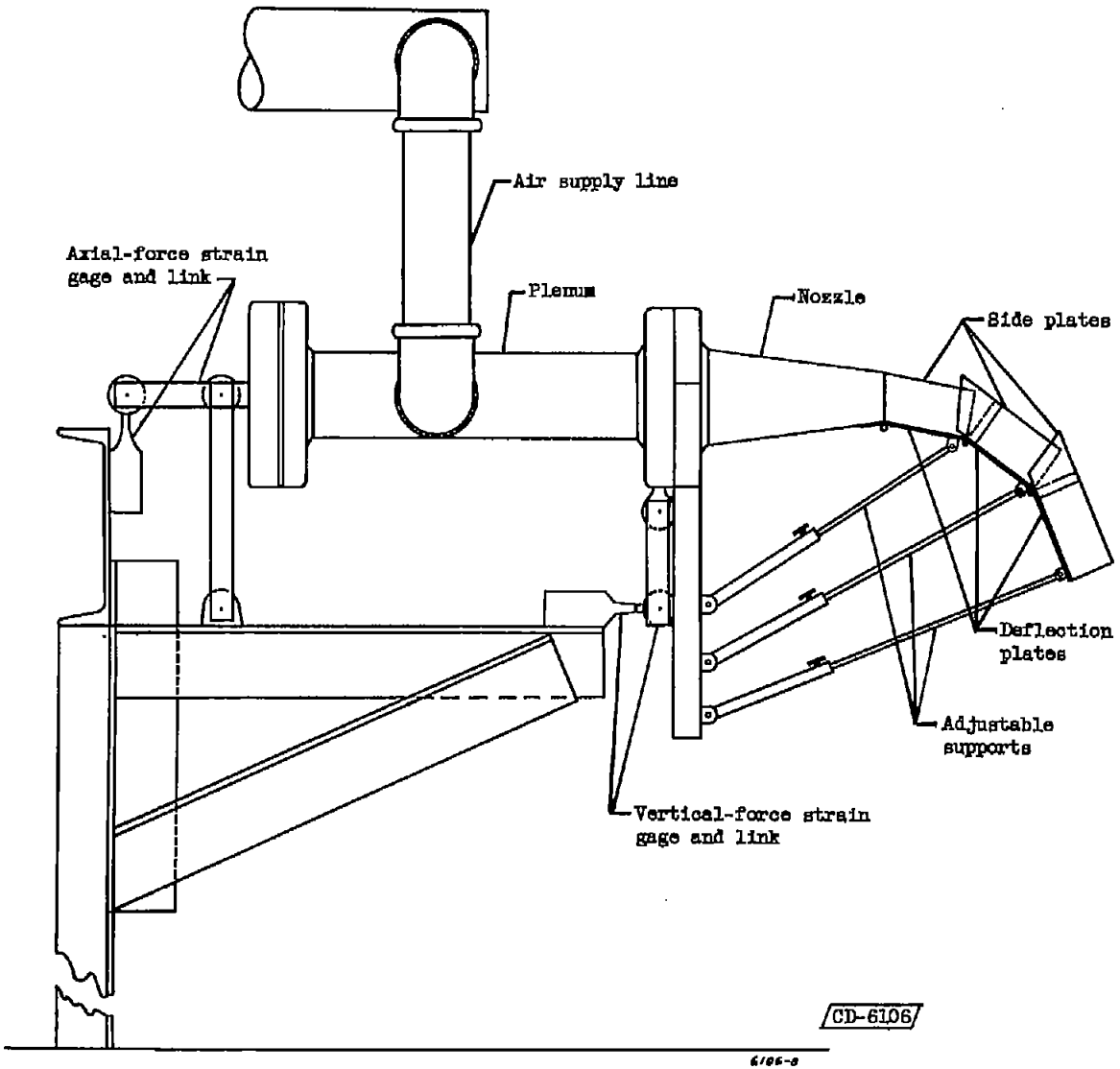

Figure 1. - Setup for Coanda nozzle tests.

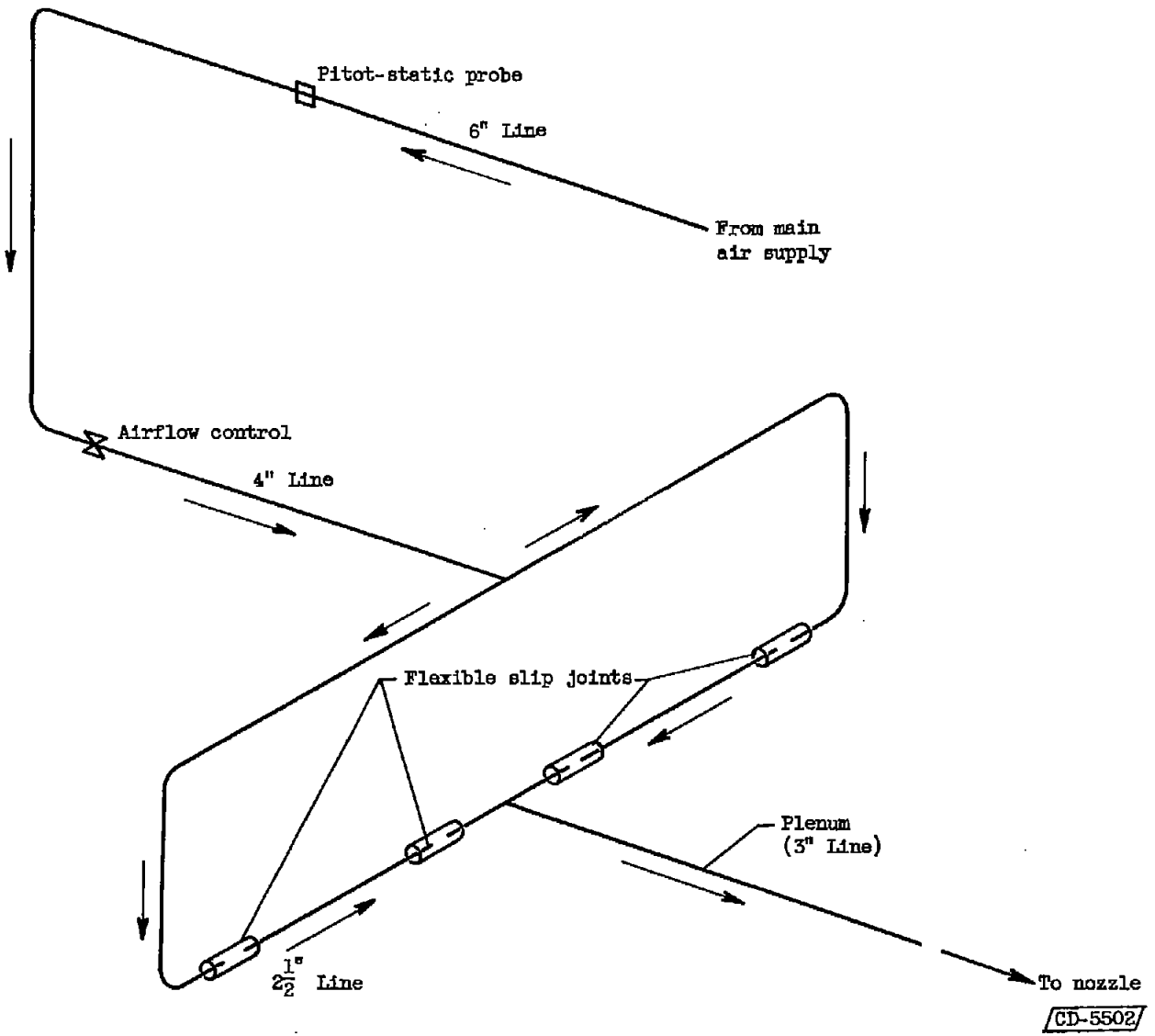

Figure 2. - Airflow in supply system.

Nozzle	Height, in.	Width, in.	Exit area, sq in.
a	0.5	4.2	2.1
b	1.1	3.7	4.1
c	2.0	2.8	5.6

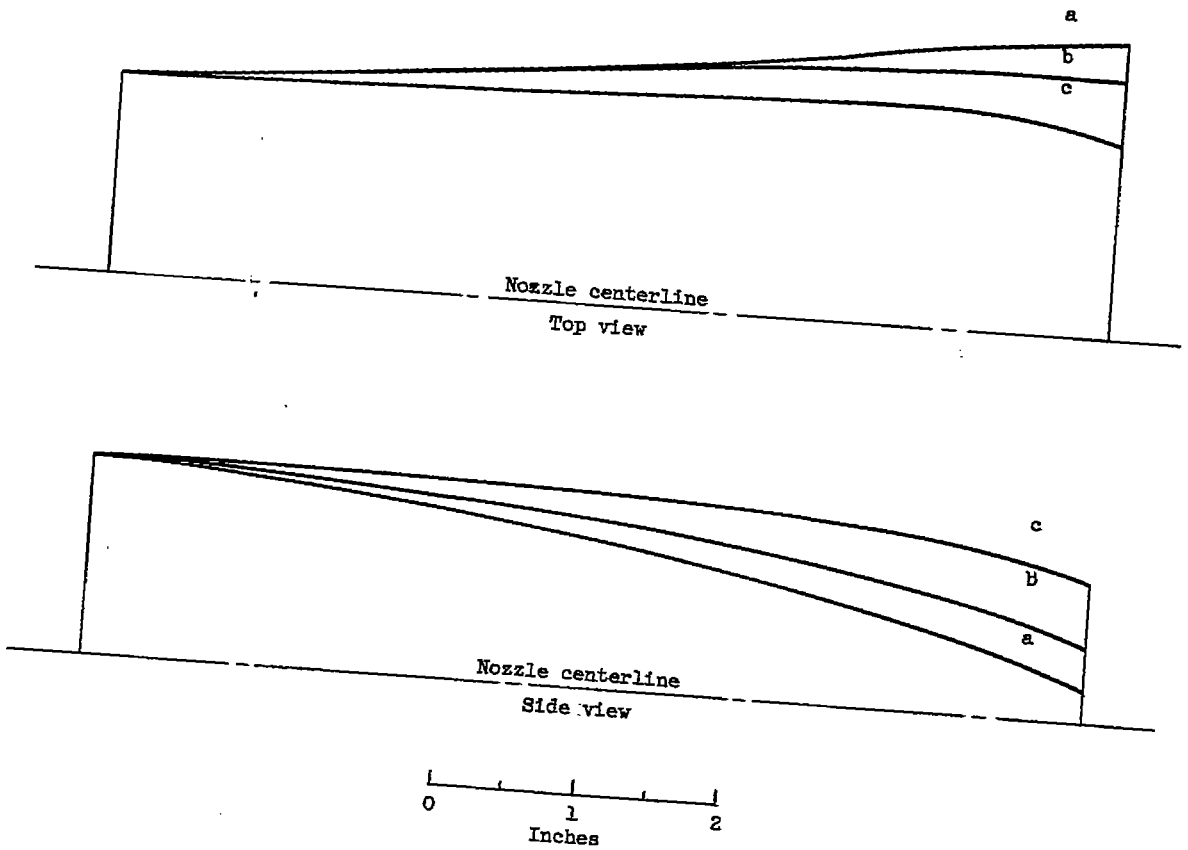

Figure 3. - Cross sections of nozzles.

Figure 4. - Typical installation of multiple-flat-plate configuration.

4807

CU-6

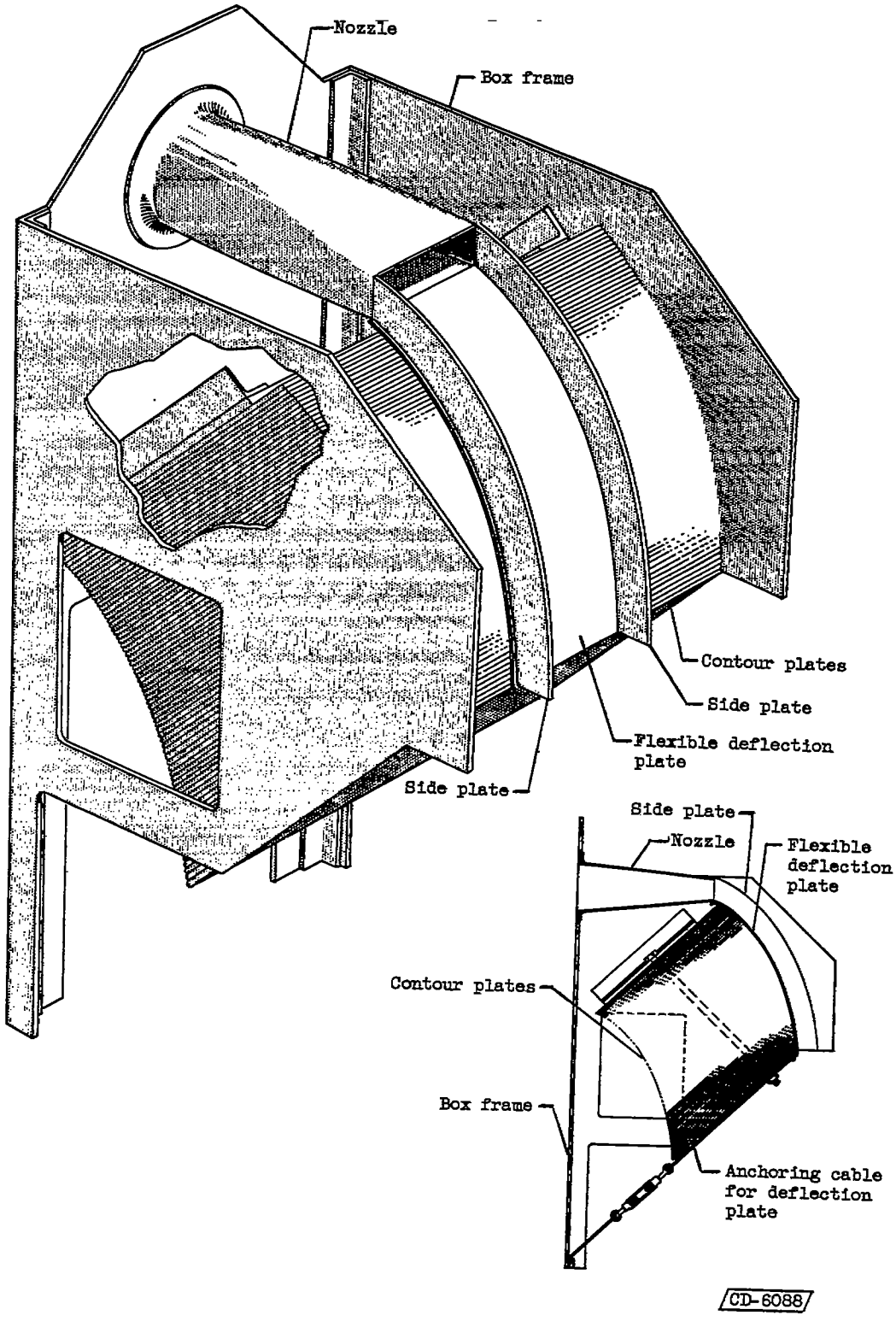

Figure 5. - Setup for Coanda nozzles using curved-plate deflectors.

4807

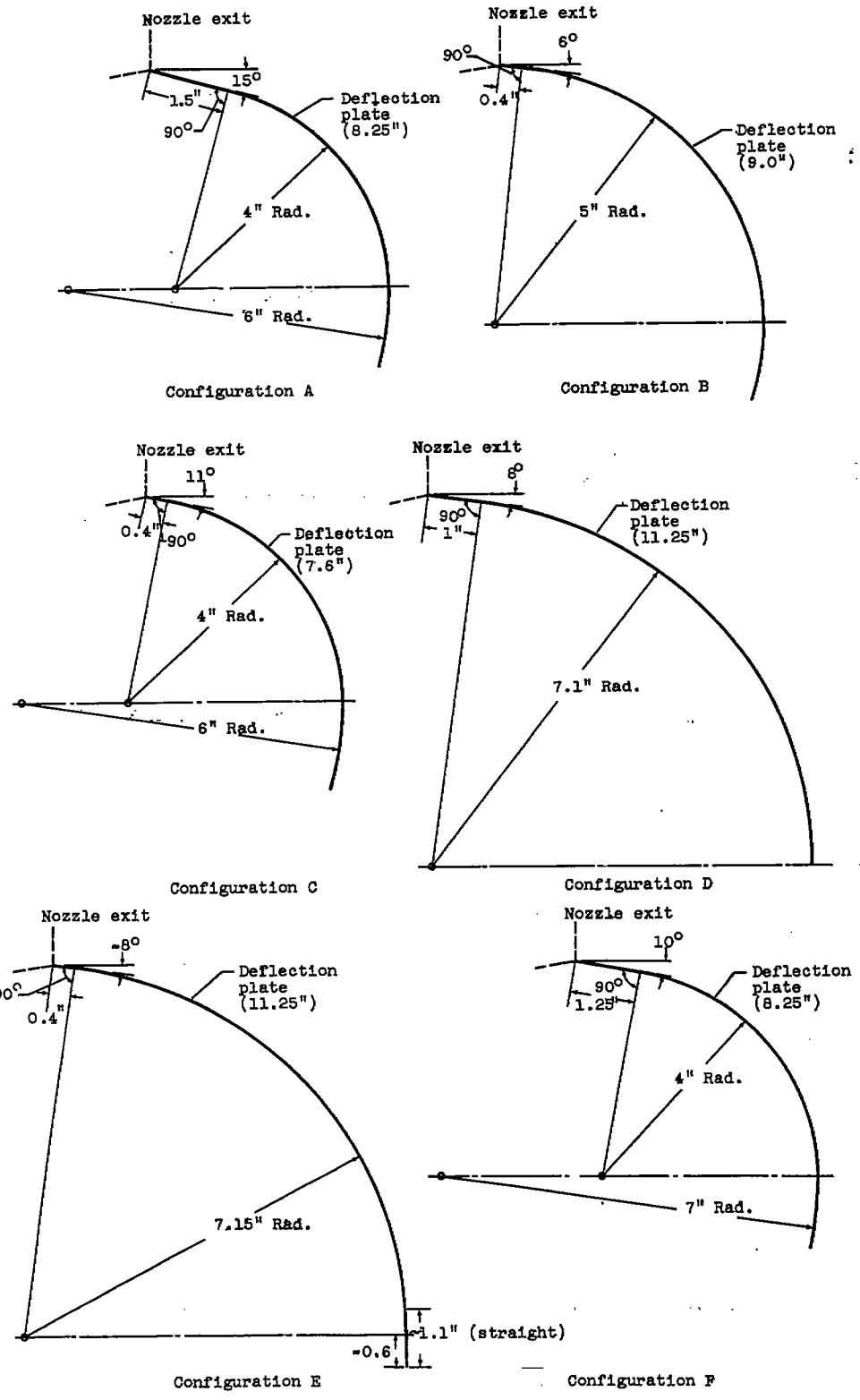

Figure 6. - Cross-sectional sketches of curved deflection plates.

4807

CU-6 back

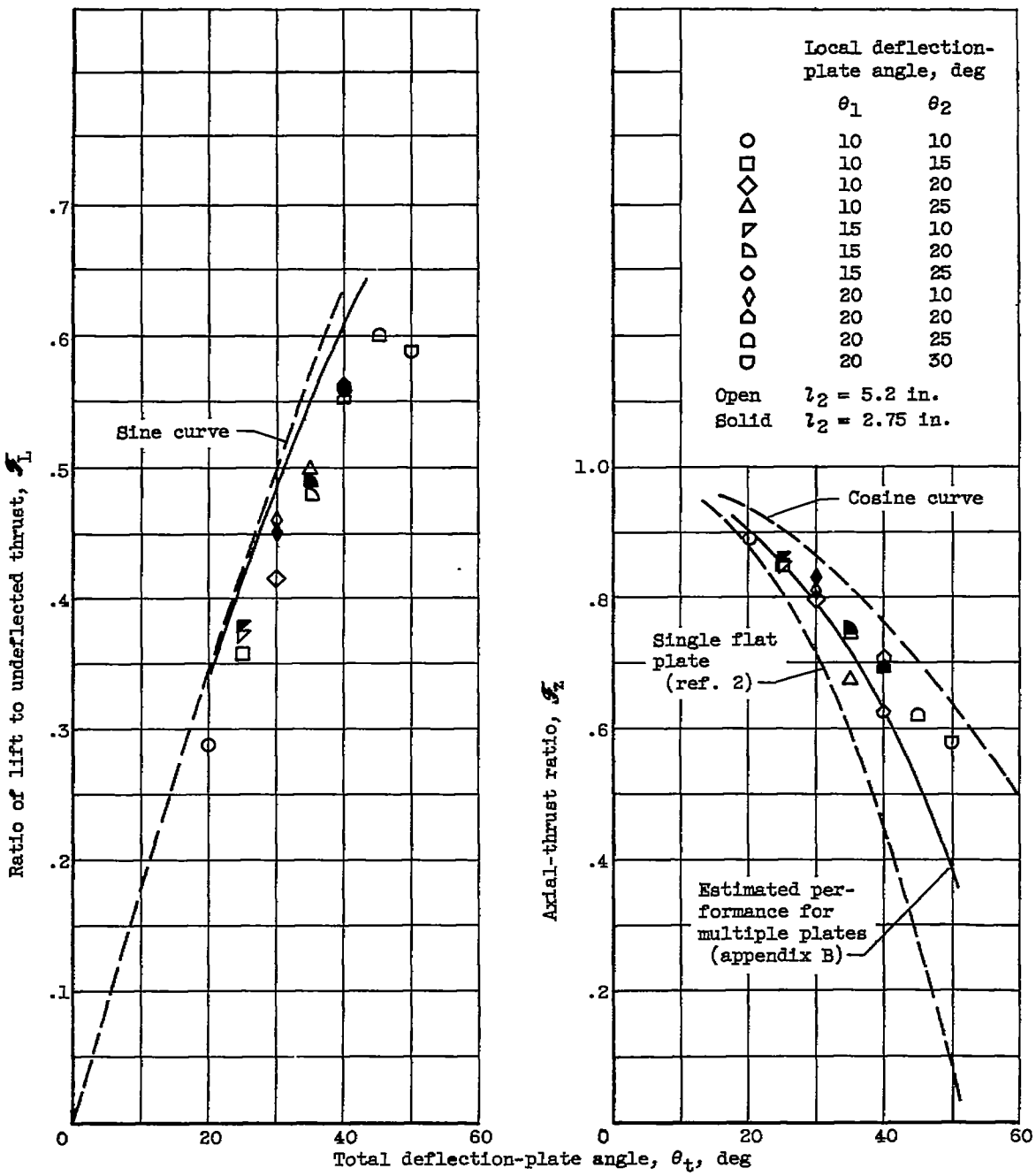

Figure 7. - Variation of two-flat-plate Coanda nozzle performance characteristics with total deflection-plate angle. Nominal pressure ratio, 2.1; nozzle height, 1.1 inches; l_1 = 2.0 inches.

4807

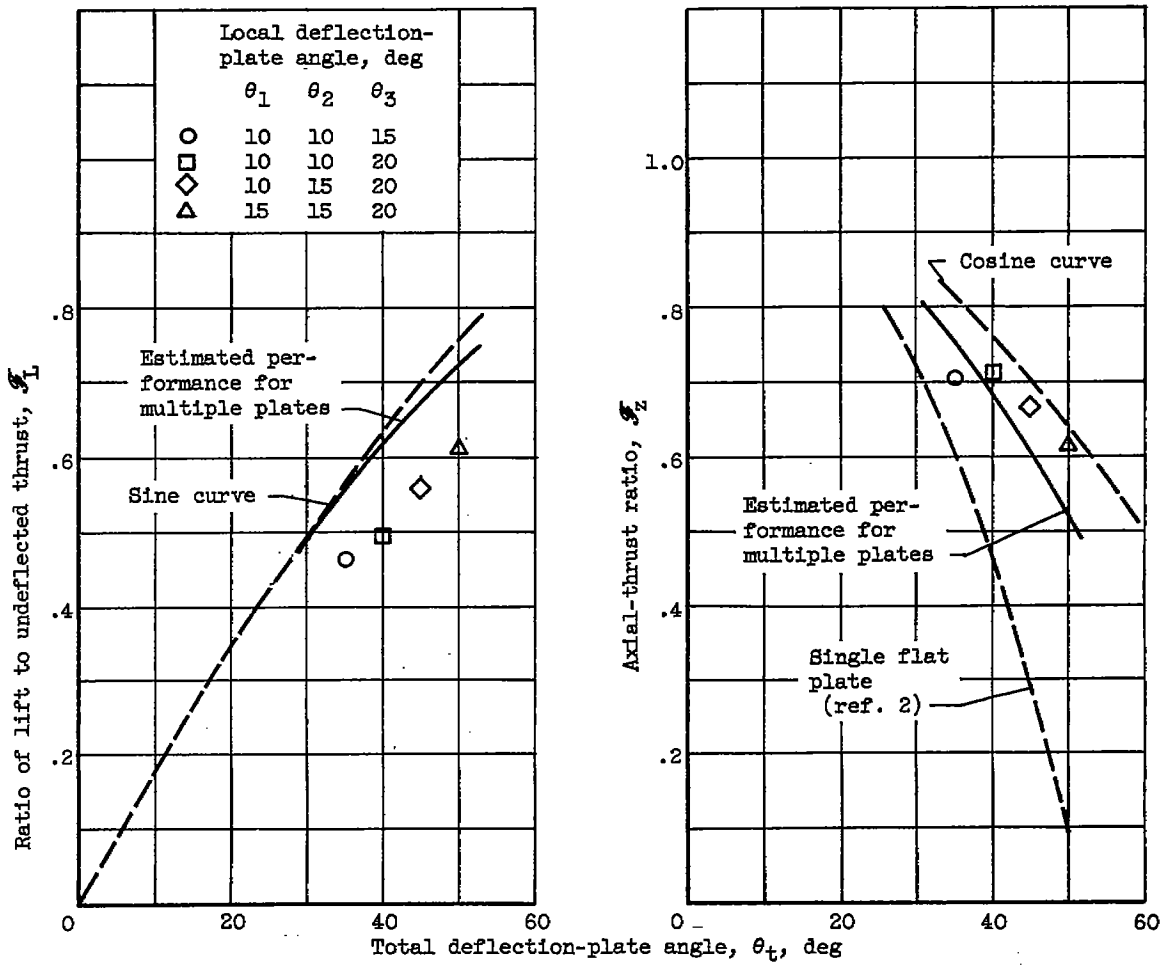

(a) Nozzle height, 2.0 inches; plate lengths: l_1 = 2.5, l_2 = 2.75, and l_3 = 4.88 inches.

Figure 8. - Variation of three-flat-plate Coanda nozzle performance characteristics with total deflection-plate angle. Nominal pressure ratio, 2.1.

4807

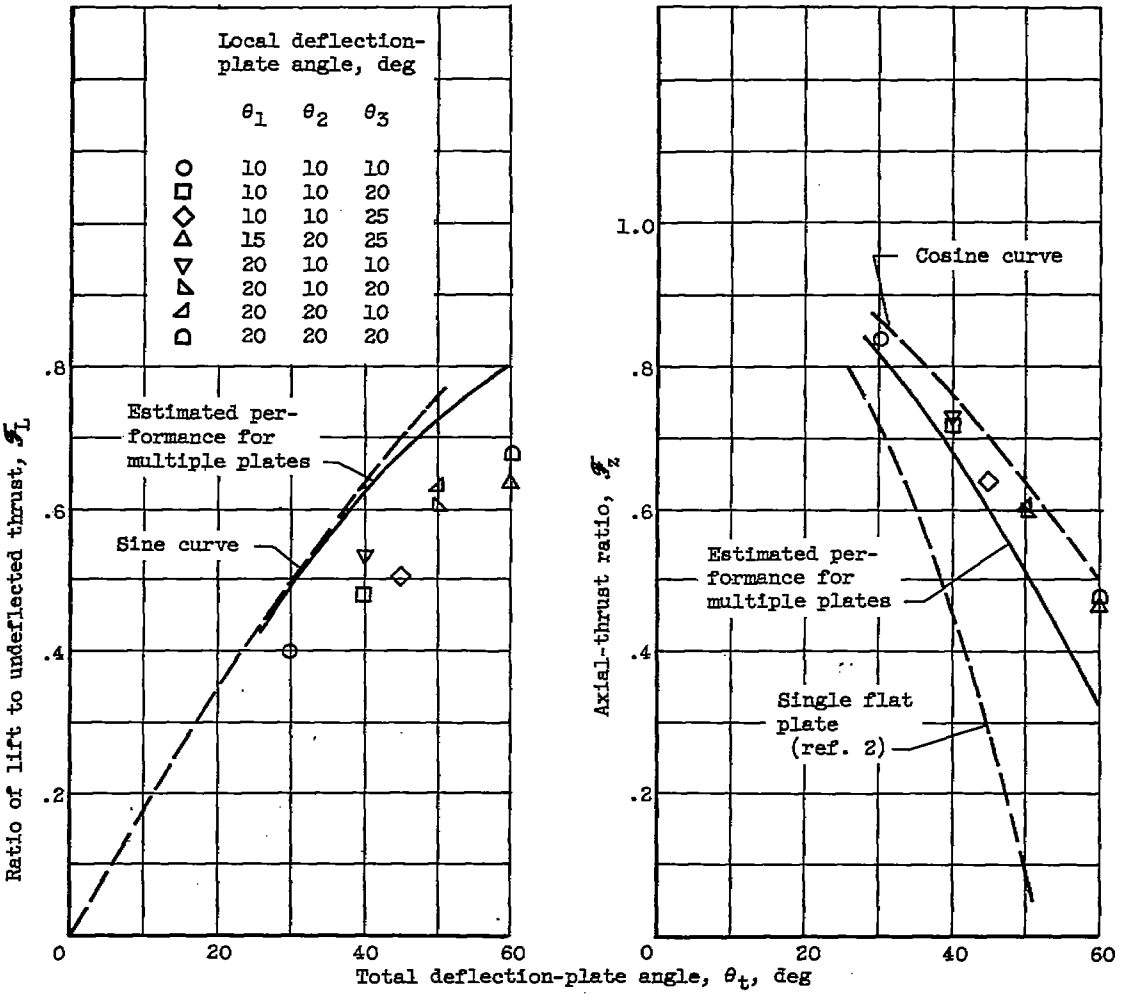

(b) Nozzle height, 1.1 inches; plate lengths: l_1 = 2.0, l_2 = 2.75, and l_3 = 4.88 inches.

Figure 8. - Continued. Variation of three-flat-plate Coanda performance characteristics with total deflection-plate angle. Nominal pressure ratio, 2.1.

4807

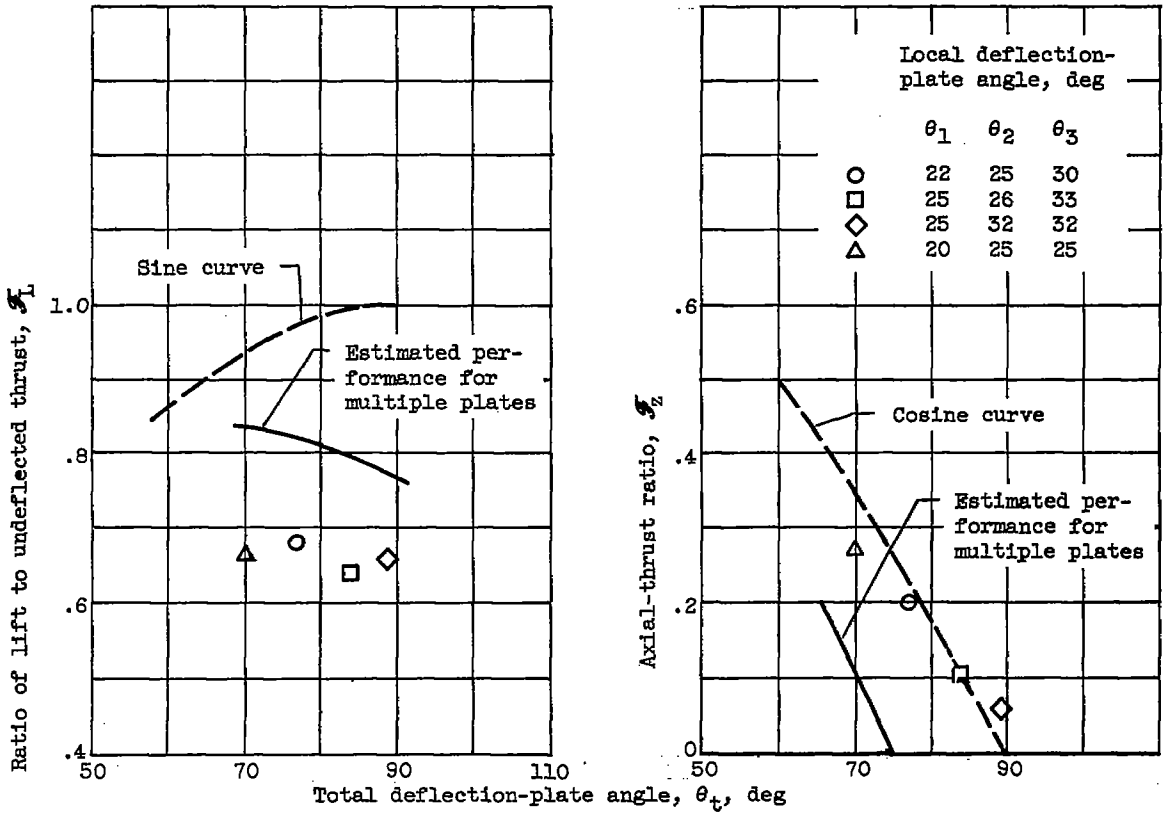

(c) Nozzle height, 0.5 inch; plate lengths: l_1 = 2.5, l_2 = 2.75, and l_3 = 4.88 inches.

Figure 8. - Concluded. Variation of three-flat-plate Coanda performance characteristics with total deflection-plate angle. Nominal pressure ratio, 2.1.

4807

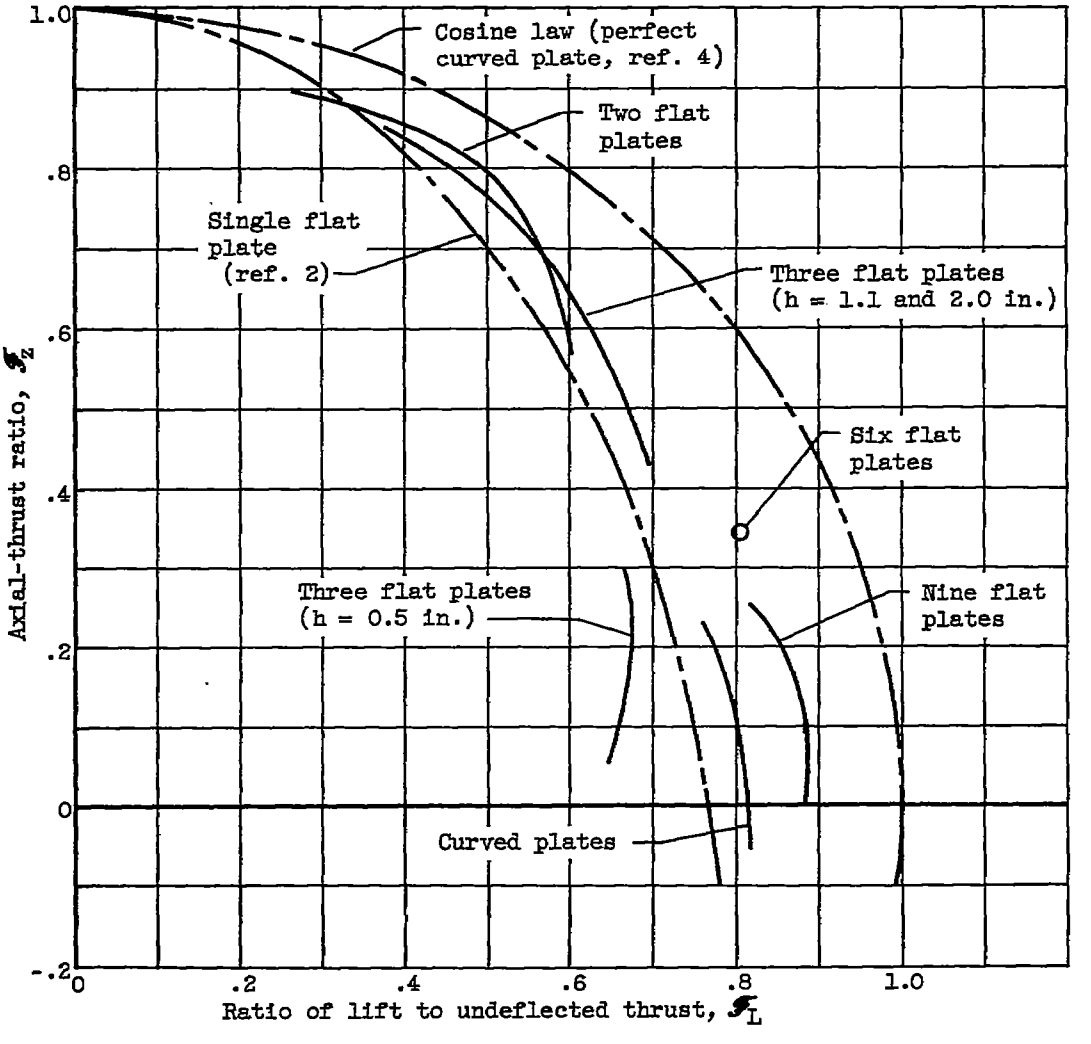

Figure 9. - Comparison of maximum performance of single-flat-plate, multiple-flat-plate, and curved-plate Coanda nozzles. Nominal pressure ratio, 2.1.

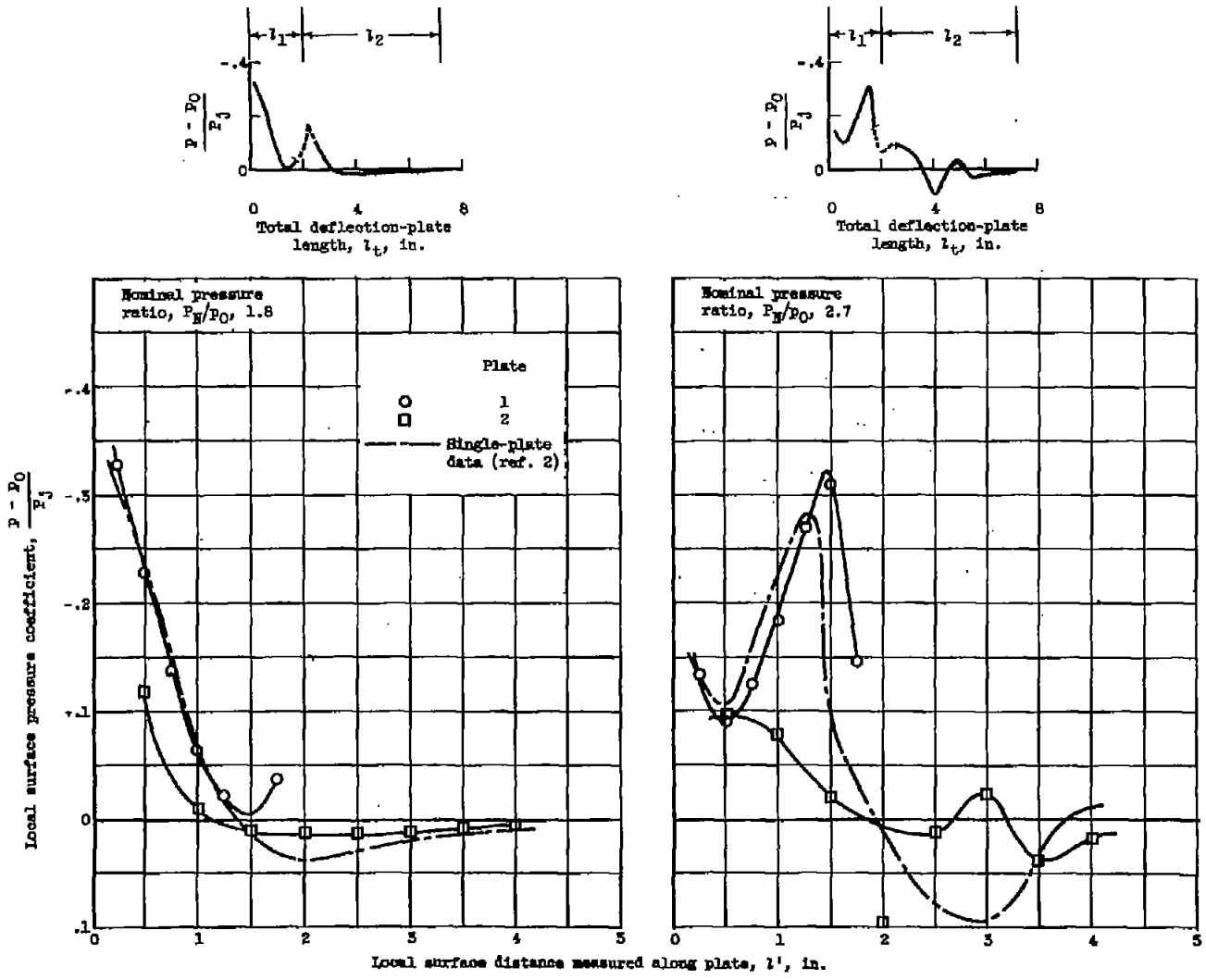

(a) Local deflection angle for each plate, 10°.

Figure 10. - Representative pressure distributions over two-flat-plate Coanda nozzle configuration for pressure ratios above and below choking. Nozzle height, 1.1 inches; plate lengths, 2.0 and 5.2 inches.

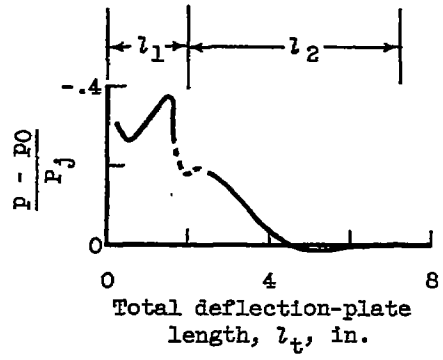

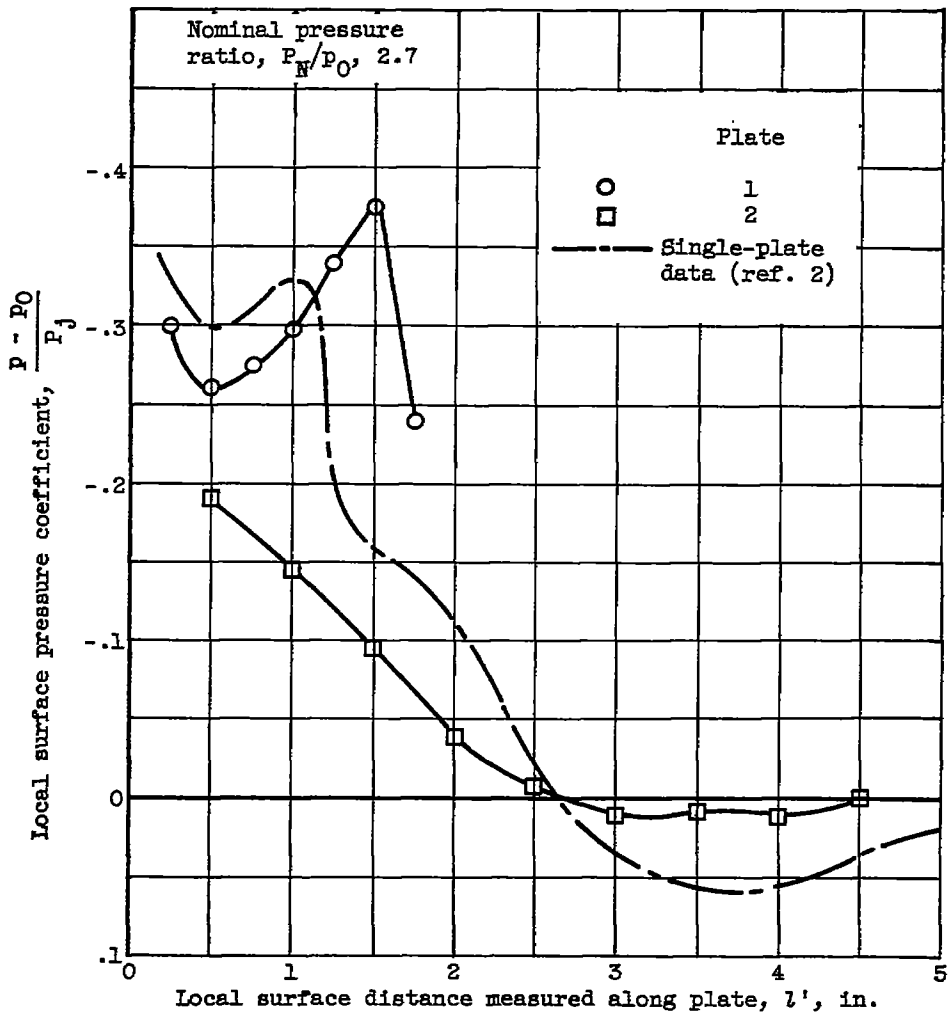

(b) Local deflection angle for each plate, 20°.

Figure 10. - Concluded. Representative pressure distributions over two-flat-plate Coanda nozzle configuration for pressure ratios above and below choking. Nozzle height, 1.1 inches; plate lengths, 2.0 and 5.2 inches.

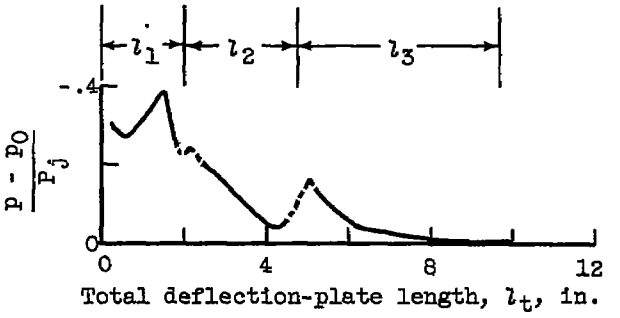

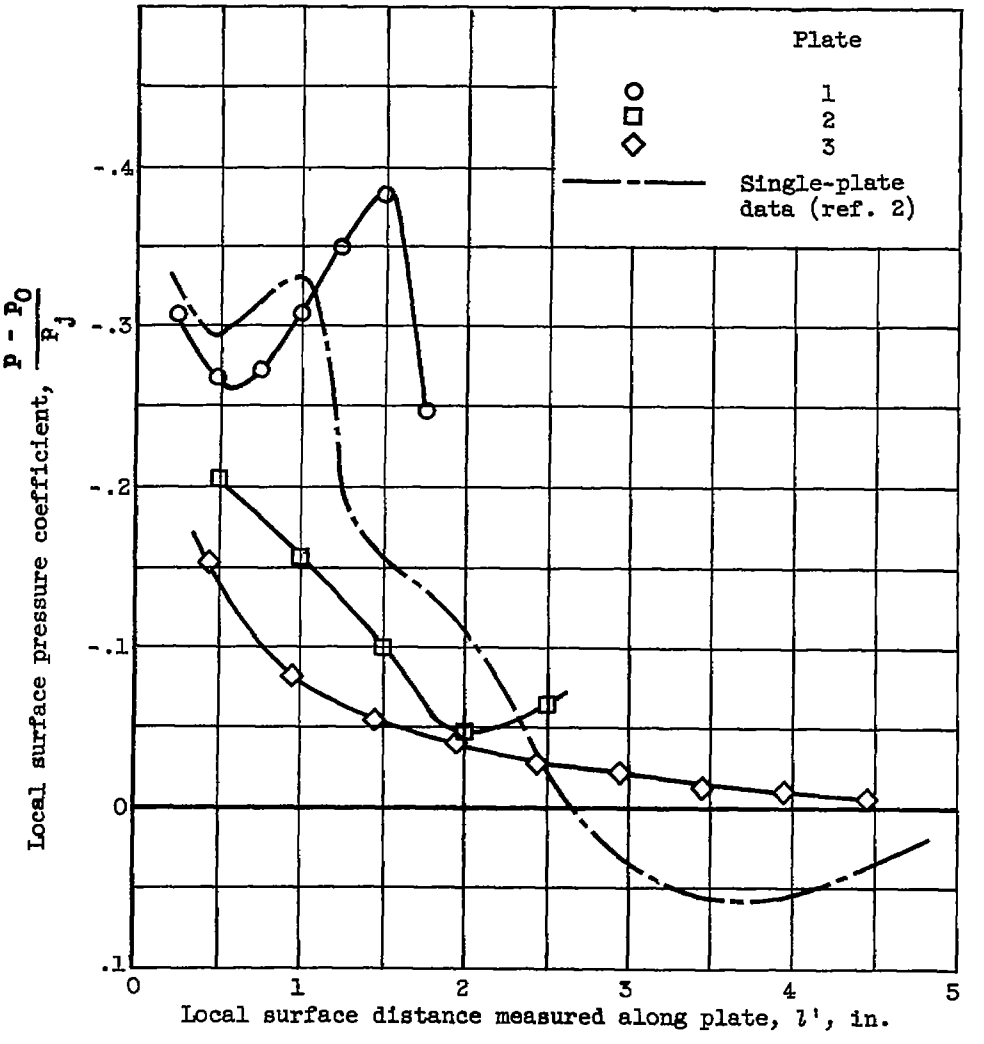

Figure 11. - Representative pressure distributions over three-flat-plate Coanda nozzle configuration. Nominal pressure ratio, 2.7; nozzle height, 1.1 inches; local deflection angle for each plate, 20°; plate lengths, 2.0, 2.75, and 4.88 inches.

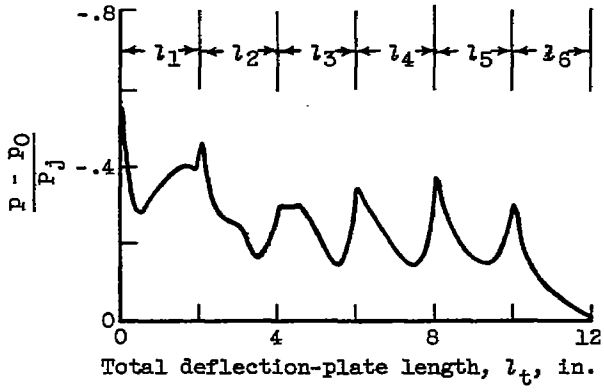

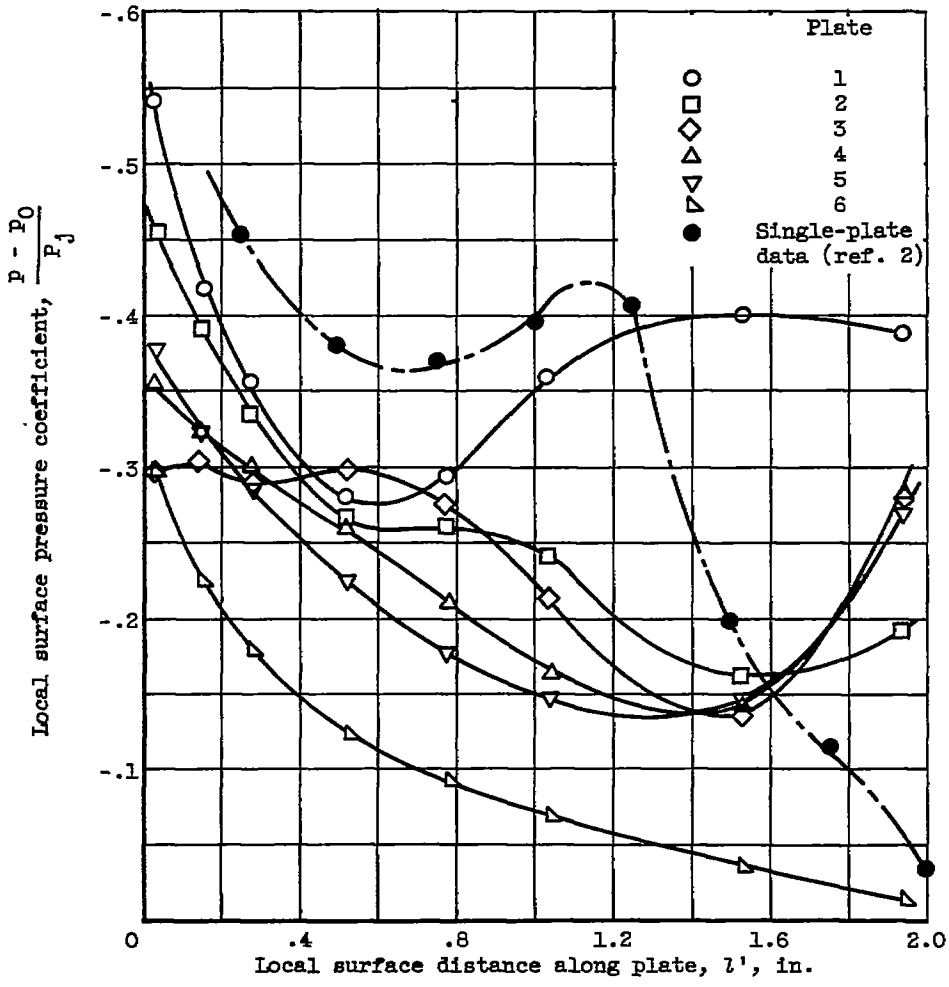

Figure 12. - Variation of surface pressure distribution with plate length for a six-flat-plate Coanda nozzle. Nominal pressure ratio, 2.4; plate lengths, 2.0 inches each; deflection angle, 12.5° each plate; nozzle height, 2.0 inches; total deflection-plate angle, 75°.

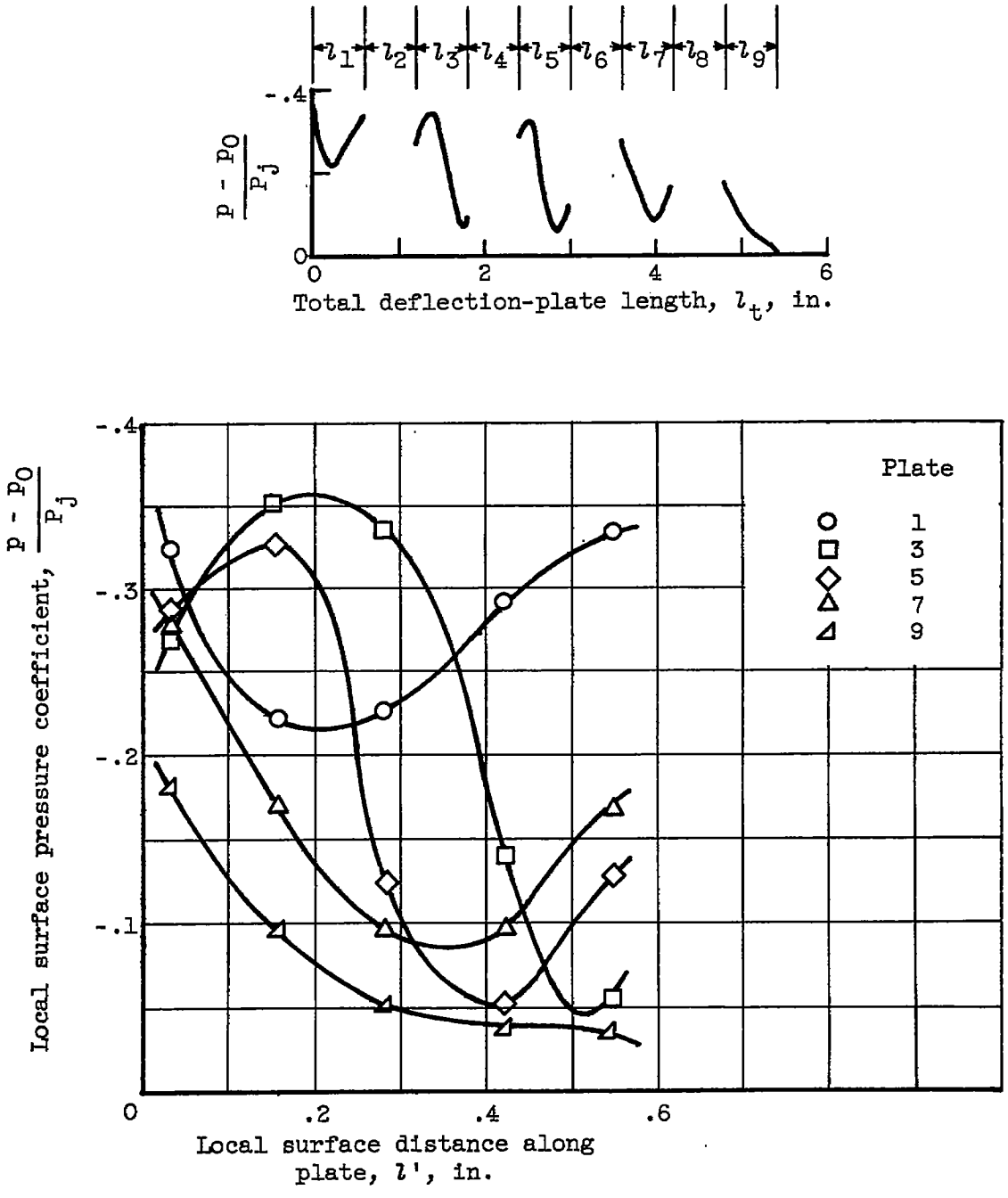

Figure 13. - Variation of surface pressure distribution with plate length for a nine-flat-plate Coanda nozzle. Nominal pressure ratio, 2.1; plate lengths, 0.6 inch each; deflection angle, 10° each plate; nozzle height, 0.5 inch; total deflection-plate angle, 90°.

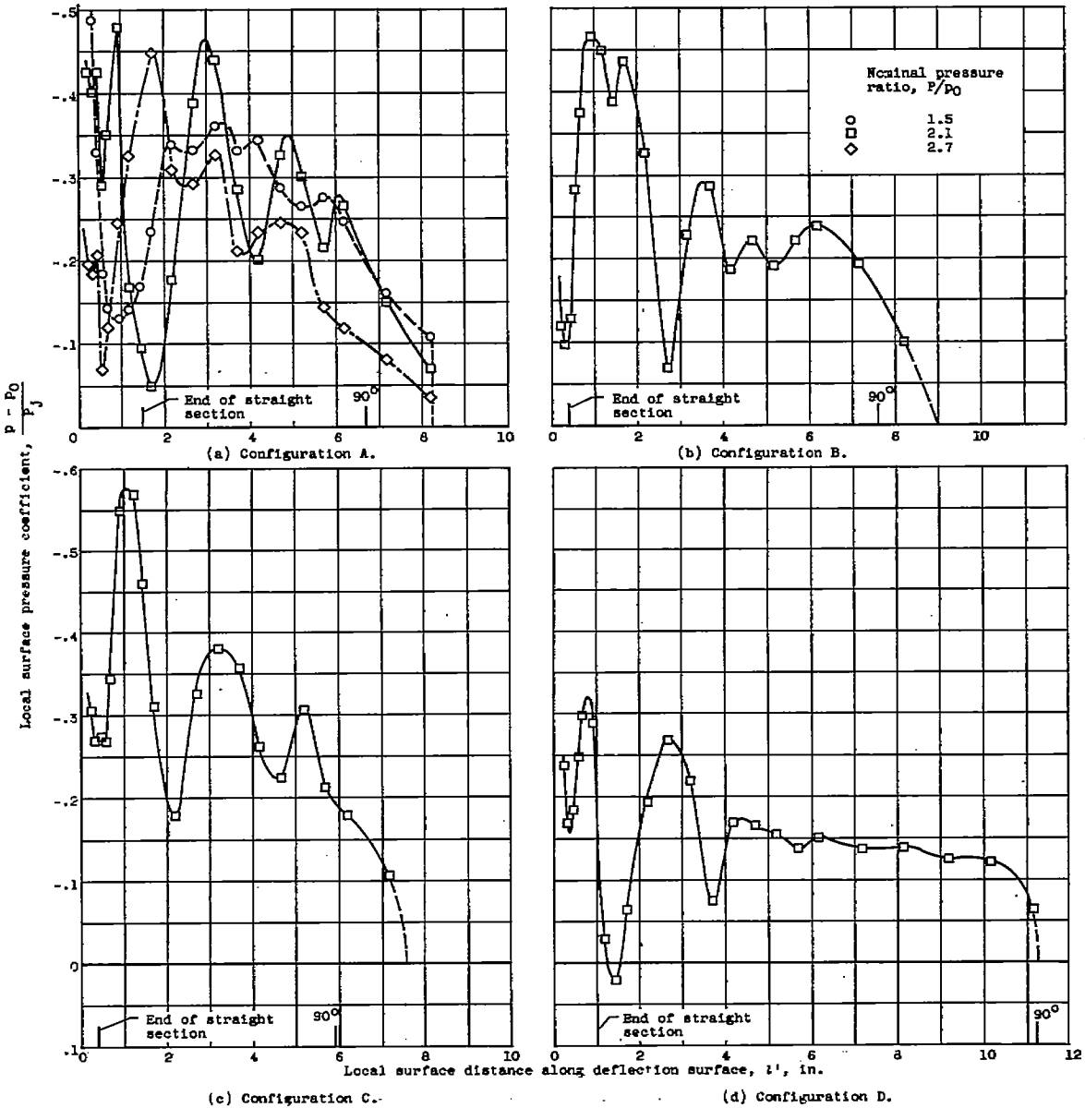

Figure 14. - Typical surface pressure distributions for Coanda nozzles with curved deflection plates. Nozzle height, 0.5 inch.

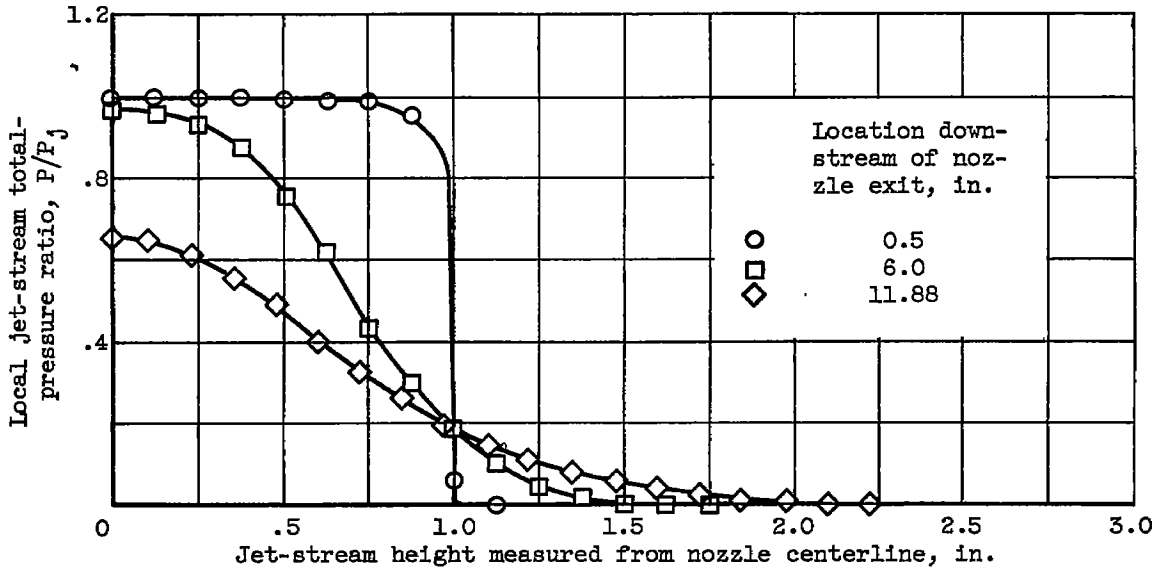

(a) Local jet-stream total-pressure profile. Nominal pressure ratio, 2.1.

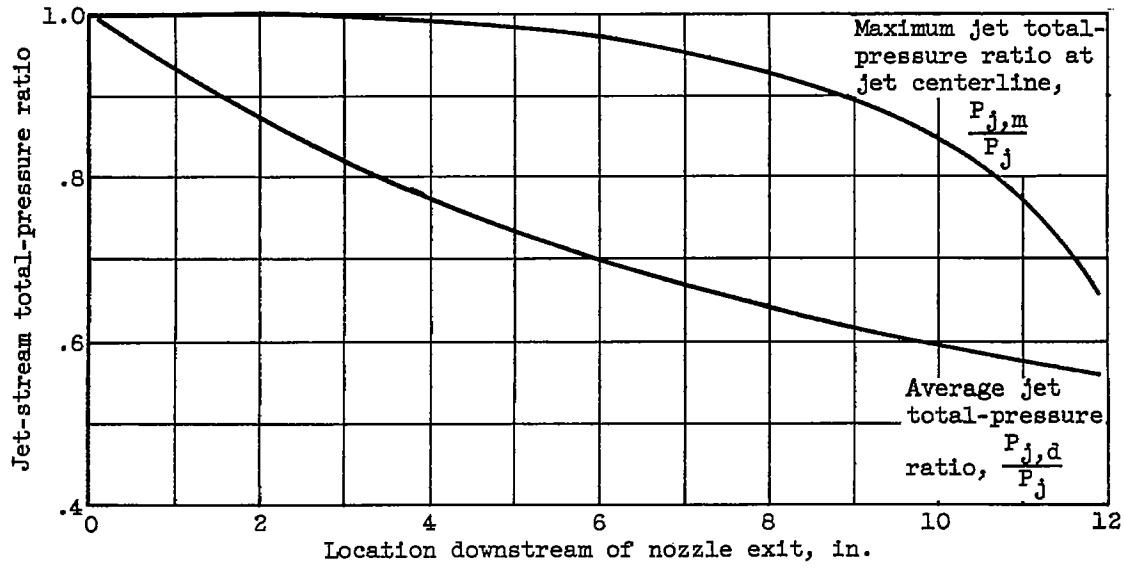

(b) Average and maximum jet-stream total-pressure ratios as function of location downstream of nozzle exit; average for nozzle pressure ratios from 1.5 to 2.7.

Figure 15. - Total-pressure characteristics of undeflected jet stream. Nozzle height, 2.0 inches.